JOURNAL OF GEOPHYSICAL RESEARCH: ATMOSPHERES, VOL. 118, 4572–4596, doi:10.1002/jgrd.50407, 2013

Seasonal and diurnal variations of aerosol extinction profile and type distribution from CALIPSO 5-year observations

Lei Huang,[1] Jonathan H. Jiang,[2] Jason L. Tackett,[3] Hui Su,[2] and Rong Fu[1]

Received 21 February 2013; revised 5 April 2013; accepted 10 April 2013; published 23 May 2013.

[1] The new Level 3 aerosol profile data derived from the Cloud-Aerosol Lidar and Infrared Pathfinder Satellite Observations (CALIPSO) provide a multiyear global aerosol distribution with high vertical resolution. We analyzed seasonal and diurnal variations of the vertical distributions of aerosol properties represented by 5-year CALIPSO data. Results show that dust, smoke, and polluted dust are the most frequently detected aerosol types during all seasons. Dust is the dominant type, especially in the middle to upper troposphere, over most areas during boreal spring and summer, while smoke and polluted dust tend to dominate during biomass burning seasons. The seasonal variations of dust layer top height and dust contribution to all-aerosol extinction are positively correlated with the seasonal variation of the dust occurrence frequency. The seasonal cycle of aerosol properties over west Australia is similar to that over biomass burning regime areas, despite its desert regime. In general, smoke is detected more frequently from the lower to middle troposphere; clean marine and polluted continental aerosols are detected more frequently, while polluted dust is detected less frequently, in the lower troposphere during nighttime than daytime. The all-aerosol extinction is generally larger, and the aerosol layer top is detected at high altitudes more frequently during nighttime than daytime. The diurnal changes of aerosol properties are similar within the same aerosol regime. Dust extinction shows little diurnal variation except when dust is the dominant aerosol type. The results contribute to an initial global 3-D aerosol climatology which will likely be extended and improved in the future.

Citation: Huang, L., J. H. Jiang, J. L. Tackett, H. Su, and R. Fu (2013), Seasonal and diurnal variations of aerosol extinction profile and type distribution from CALIPSO 5-year observations, *J. Geophys. Res. Atmos.*, *118*, 4572–4596, doi:10.1002/jgrd.50407.

1. Introduction

[2] Aerosols play a number of important roles in modern climate change and atmospheric composition. Aerosols exert a strong influence on the atmospheric energy budget and therefore climate, primarily through two mechanisms: a radiative (direct) effect and a microphysical (indirect) effect. The aerosol radiative effect is associated with the scattering and absorption of solar radiation [e.g., *Charlson et al.*, 1992]. Scattering acts to cool the air, while absorption acts to warm it. Absorbing aerosols, such as black carbon and mineral dust, can cause substantial diabatic heating in the atmosphere, which can enhance cloud evaporation or inhibit cloud formation [e.g., *Ackerman et al.*, 2000; *Koren et al.*, 2004]. The aerosol microphysical effect is associated with aerosols serving as cloud condensation nuclei and ice nuclei [*Twomey*, 1977], which can modify the size distribution of cloud droplets and ice particles. These modifications affect internal cloud microphysics, cloud radiative properties and precipitation efficiency, and, by extension, the atmospheric hydrological cycle and energy balance [e.g., *Jiang and Feingold*, 2006; *Jiang et al.*, 2008]. Both the radiative and microphysical effects of aerosols can have complicated impacts on weather and climate systems [e.g., *Koren et al.*, 2008]. Taken together with incomplete knowledge of the physical and chemical properties of aerosols and their spatial and temporal distributions, these aerosol effects represent major sources of uncertainty in both the attribution of past climate changes and the prediction of future climate changes [*Intergovernmental Panel on Climate Change (IPCC)*, 2007]. The estimates of the aerosol direct radiative forcing on climate in the Intergovernmental Panel on Climate Change (IPCC) Fourth Assessment Report are largely based on climate model simulations, partly due to the fact that aerosol observations were inadequate and had large uncertainties. Evaluating and characterizing aerosol impact on climate requires high resolution (both horizontally and vertically) and long-term continuous observations of aerosols, which have large temporal and spatial variations.

[1]Department of Geological Sciences, Jackson School of Geosciences, The University of Texas at Austin, Austin, Texas, USA.
[2]Jet Propulsion Laboratory, California Institute of Technology, Pasadena, California, USA.
[3]Science Systems and Applications, Inc., Hampton, Virginia, USA.

Corresponding author: L. Huang, Department of Geological Sciences, University Station C1100, The University of Texas at Austin, Austin, TX 78712, USA. (leih@utexas.edu)

2169-897X/13/10.1002/jgrd.50407

[3] The vertical variability of aerosols in the atmosphere has been less well studied than the horizontal variability, largely because it is more difficult to sample aloft than from a ground-based platform. However, the vertical profiles of aerosol played an important role in determining aerosol radiative forcing. For example, *Haywood and Ramaswamy* [1998] argued that the vertical distribution of aerosols is important in determining the magnitude and sign of aerosol direct radiative forcing. More recently, *Rozwadowska* [2007] have found that errors in the assumptions about the shape of aerosol profiles can cause errors in satellite retrieval of aerosol optical thickness. Meanwhile, many previous analyses of aerosol vertical distributions were confined to small spatial scales with focus on a specific city or region due to coverage limitations [e.g., *Li et al*., 1997; *Osborne and Haywood*, 2005; *Hains et al*., 2008]. Aircraft missions are still used today to collect aerosol samples and measure aerosol size distributions [*Kaufman et al*., 2003; *Shinozuka et al*., 2007; *Liu et al*., 2009a], and ground-based lidar data [e.g., *Chazette*, 2003; *Matthias et al*., 2004; *Huang et al*., 2010] are still necessary to examine vertical profiles of aerosol extinction as most satellite data are restricted to column values or averages. However, due to continued advancement of remote sensing technology, new tools are becoming available to study aerosol profiles.

[4] The new aerosol profile data derived from the Cloud-Aerosol Lidar and Infrared Pathfinder Satellite Observations (CALIPSO) provide an opportunity to assess model simulations of aerosol vertical distributions on global and annual scales. Since the launch of CALIPSO, various methods have been employed to use the data. For example, the CALIPSO data have been used in concert with model simulations and other satellite instruments to evaluate aerosol vertical distributions [*Huang et al*., 2009; *Bou Karam et al*., 2010; *Yu et al*., 2010], validate model simulations [*Generoso et al*., 2008], and assimilate observations into models to correct for nonhomogeneous background error statistics [*Sekiyama et al*., 2010]. *Yu et al*. [2010] examined seasonal variations of aerosol vertical distributions through an analysis of 18-month CALIPSO data and compared with model aerosol simulations as well as aerosol optical depth (AOD) measurements from the Moderate Resolution Imaging Spectroradiometer. However, their work mainly focused on comparisons between satellite observations and model simulations of aerosol optical property and did not include aerosol type distribution and diurnal variations of aerosol properties. Despite previous efforts to evaluate aerosol vertical distributions, a lack of assessment of global, climatological, as well as diurnal variations of aerosol vertical distributions still exists.

[5] Given the current need for a better understanding of the vertical distributions and variations of aerosols in order to quantify aerosol effects on climate change and the hydrological cycle through model simulation, this study aims to: (1) analyze climatological regional and seasonal variations of the vertical distribution of aerosol optical and type properties using 5-year CALIPSO observations and (2) evaluate diurnal variations of the vertical distribution of different aerosol properties. The rest of this paper is organized as follows: a brief description of CALIPSO measurements, Level 3 aerosol data, and quality information are given in section 2. The climatological seasonal variations of aerosol extinction and type profiles, as well as the maximum aerosol layer top altitudes, in different aerosol regime regions are presented and discussed in section 3. Section 4 discusses the diurnal variations of aerosol vertical distributions. Major findings and conclusions are summarized in section 5.

2. Data Sets

[6] The CALIPSO satellite was launched into a Sun-synchronous orbit on 28 April 2006 with a local equator-crossing time of about 1:30 P.M. and 1:30 A.M., with a 16-day repeating cycle. The primary instrument on board CALIPSO is the Cloud-Aerosol Lidar with Orthogonal Polarization (CALIOP), which is a dual-wavelength polarization lidar designed to acquire vertical profiles of attenuated backscatter from a near nadir-viewing geometry during both day and night phases [*Winker et al*., 2007]. Since then, it has become one member of the A-Train [*L'Ecuyer and Jiang*, 2010] satellite constellation and has been collecting almost continuously high-resolution (333 m in the horizontal and 30 m in the vertical below 8.3 km) profiles of the attenuated backscatter by aerosols and clouds at 532 and 1064 nm wavelengths along with polarized backscatter at 532 nm between 82°N and 82°S [*Winker et al*., 2007]. Spatial averaging over different scales is usually taken to improve the signal-to-noise ratio (SNR) for reliable aerosol retrieval.

[7] The features identified by CALIPSO are first classified into aerosol and cloud using a cloud-aerosol discrimination (CAD) algorithm [*Liu et al*., 2009b]. The level of confidence in the aerosol-cloud classification is reflected by a CAD score, with negative values (−100 to 0) for aerosol and positive values (+100 to 0) for cloud. The larger absolute value of this score represents the higher confidence of the feature classification. After an aerosol layer is identified, the scene classification algorithm further categorizes the aerosol layer to one of six aerosol types by using input parameters, including altitude, location, surface type, volume depolarization ratio, and integrated attenuated backscatter measurements [*Omar et al*., 2009]. The six aerosol types are smoke (biomass burning aerosol), polluted continental (urban/industrial pollution), polluted dust (mixture of dust and smoke), dust (desert), clean continental (clean background), and clean marine (sea salt). Each aerosol type has a preassigned lidar ratio (or an extinction-to-backscatter ratio) which is later used in the retrieval of aerosol extinction. More details can be found in recent papers [e.g., *Liu et al*., 2009b; *Omar et al*., 2009; *Young and Vaughan*, 2009; *Winker et al*., 2009].

[8] Aerosol extinction is retrieved by the Hybrid Extinction Retrieval Algorithms using the assumed lidar ratios appropriate for each aerosol type [*Young and Vaughan*, 2009] and reported in the CALIPSO Level 2, 5-km aerosol profile product. The determination of lidar ratio is one of the major factors affecting the uncertainty of CALIPSO aerosol extinction retrieval, and the misclassification of aerosol type is another source of uncertainty [*Yu et al*., 2010]. In addition, another important source of uncertainty in the aerosol profile retrieval occurs when the base of the aerosol layer is incorrectly identified (e.g., above the true layer base). To compensate for cases where the aerosol layer base is identified too

high, a "Layer Base Extension" algorithm has been adopted in CALIPSO Level 2 Version 3.0 retrieval that extends the base of the lowest aerosol layer in the column to 90 m above the local surface for layers having positive mean attenuated backscatter 532 nm that are within 2.5 km of the surface [*CALIPSO*, 2010]. The assumption is that boundary layer aerosols are often surface attached and extending the base allows the usable signal below the original base to contribute to column AOD, reducing the low AOD bias. Moreover, if the aerosol attenuated backscatter signal is below the instrument sensitivity of $2–4 \times 10^{-4}$ $km^{-1}sr^{-1}$ in the troposphere [*Winker et al*., 2009], CALIOP will miss such features. Because retrieval errors propagate downward, the lower parts of the aerosol profile always have higher uncertainty and may contain more retrieval artifacts. The CALIOP is less sensitive during daytime than nighttime due to SNR reduction by solar background illumination [*Liu et al*., 2009b]; thus, weakly scattering (or optically thin) layers which are detected during nighttime may be missed during daytime. It is important to keep this fact in mind when interpreting diurnal variations in the occurrence frequency of aerosol type and maximum aerosol layer top altitude.

[9] The CALIPSO Version 3.0 Level 2 data products have significant improvements over previous versions, which have been demonstrated by previous validation studies [e.g., *Kacenelenbogen et al*., 2011; *Redemann et al*., 2012; *Koffi et al*., 2012]. In this study, we use the recently released CALIPSO Version 1.0 Level 3 aerosol profile data, a globally gridded monthly product derived from CALIPSO Version 3.0 Level 2, 5-km aerosol profile product [*Powell et al*., 2011]. The Level 2 aerosol profile data are first quality screened and then aggregated onto a global $2° \times 5°$ latitude-longitude grid. The vertical resolution is 60 m, from −0.4 to 12.1 km above mean sea level (amsl), with a total of 208 layers [*Powell et al*., 2011]. Averaged profile data after quality screening are reported for all-aerosol (regardless of type) and for mineral dust aerosol only. Classification of dust is based on the aerosol type flags in the Level 2 profile data. Aerosol type information from Level 2 data is also reported in Level 3 as histograms of aerosol type for each latitude/longitude/altitude grid cell, including all six aerosol types. Depending on the sky condition (combined, i.e., cloud-free + above cloud, or all-sky) and lighting condition (daytime or nighttime), there are four different types of Level 3 data files. The primary variables included in these data are vertical profiles of the aerosol extinction coefficient at 532 nm, aerosol type, spatial distribution, and AOD.

[10] The quality screening strategy adopted in Level 3 data production used several filters designed to eliminate samples and layers that were detected or classified with very low confidence or that have unreliable extinction retrievals. These filters include quality control (QC) flags contained in the Level 2 data (e.g., CAD score, extinction QC, and extinction uncertainty) and newly developed filters (e.g., misclassified cloud filter) [*CALIPSO*, 2011]. Only aerosol layers having a CAD score between −100 and −20 are used in Level 3 data. However, sources of uncertainty or biases can still exist, including possible low bias near the surface, surface contamination, weaker SNR at daytime, and incorrectly assumed lidar ratio. Currently, the CALIPSO science team cautions Level 3 data users against physical interpretation of near-surface aerosol extinction (within 180 m of the local surface), which may be compromised by surface contamination errors [*CALIPSO*, 2011]. Thus, the analyses in this paper ignore samples within 180 m of the maximum surface elevation in attempts to remove these errors, though we still suggest treating extinction reported in the lowest range bin with caution. As mentioned above, daytime signals can be affected by background sunlight, reducing SNR, and feature detection sensitivity, especially in the upper level. Therefore, aerosol extinction in the upper troposphere is underestimated in the Level 3 data product due to misdetection of optically thin aerosol [*Winker et al*., 2012]. This not only impacts mean aerosol extinction profiles at higher altitudes shown in this paper, but also impacts diurnal comparisons of the occurrence frequency of aerosol type and maximum layer top altitude. Thus, the results of aerosol diurnal variation shown in this paper are preliminary, although observations associated with possible natural diurnal variability are noted. An important contributor to the uncertainty in CALIPSO Level 3 aerosol extinction statistics is the assumed lidar ratios adopted for the various aerosol types. The lidar ratio typically varies by about 30% for a given aerosol type, and different types have different magnitudes of variability [*Omar et al*., 2009; *Yu et al*., 2010]. Incorrect aerosol type classification can affect Level 3 mean aerosol extinction. For example, if a feature that is actually smoke is misclassified as clean marine, the extinction will be too small by over a factor of 3. The frequency of aerosol type misclassification and its impact on Level 3 aerosol extinction has not been quantified and is currently under investigation. Despite these uncertainties, *Winker et al*. [2012] have shown that these Level 3 aerosol data are realistic and representative for aerosol extinction greater than about 0.001 km^{-1} and up to an altitude of 4–6 km in most cases. Thus, in the following analyses, we use 0.001 km^{-1} as the lowest bound of aerosol extinction detected by CALIPSO and only discuss aerosol extinction larger than this value.

[11] The time period we used is from March 2007 to February 2012, for a total of 5 years. Because of their better SNR compared to the daytime measurements, only CALIPSO nighttime measurements at 532 nm will be used to analyze climatological regional and seasonal variations of the vertical distribution of aerosol optical and type properties. We use all-sky data in this study. The seasonal vertical profiles of aerosol extinction are calculated based on each domain average, i.e., the average of all grid cells included within each domain box.

3. Seasonal Variation of the Vertical Distribution of Aerosol Properties

[12] In order to characterize the regional difference of the aerosol distribution, we choose 13 domains and divide them into four groups according to their aerosol regimes (Figure 1). The *first group* includes South America (SAM, 80°W–40°W, 25°S–5°N), southern Africa (SAF, 0°E–50°E, 25°S–15°N), and Southeast (SE) Asia (SEA, 100°E–160°E, 15°S–15°N), where biomass burning aerosols dominate; the *second group* includes northern Africa (NAF, 15°W–60°E, 15°N–35°N), west China (WCN, 70°E–105°E, 31°N–45°N), and west Australia

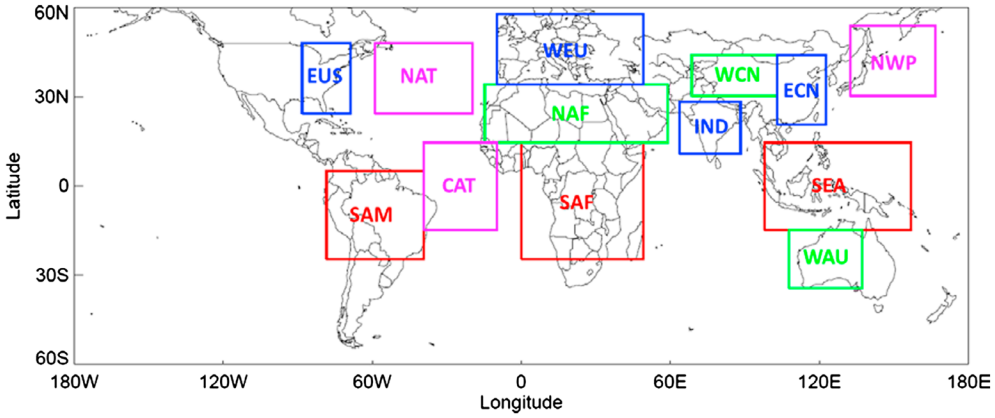

Figure 1. Thirteen domains selected for regional analysis in this study. Red boxes indicate biomass burning regime areas (South America, southern Africa, and Southeast Asia), green boxes indicate desert regime areas (northern Africa, west China, and west Australia), blue boxes indicate fossil fuel and industry regime areas (India, east China, west Europe, and East U.S.), and purple boxes indicate oceanic regime areas (northwest Pacific, North Atlantic, and central Atlantic). See text for the latitude and longitude range of each domain.

(WAU, 110°E–140°E, 15°S–35°S), comprising large desert areas; the *third group* includes India (IND, 65°E–90°E, 11°N–29°N), east China (ECN, 105°E–125°E, 21°N–45°N), west Europe (WEU, 10°W–50°E, 35°N–59°N), and East U. S. (EUS, 90°W–70°W, 25°N–49°N), where fossil fuel burning and industry generated aerosols are most common; the *fourth group* includes northwest (NW) Pacific (NWP, 135°E–170°E, 31°N–55°N), North Atlantic (NAT, 60°W–20°W, 25°N–49°N), and central Atlantic (CAT, 40°W–10°W, 15°S–15°N), which are oceanic regions located downwind of major dust and industrial pollution sources. The African savanna region to the north of the equator is an important biomass burning region [e.g., *Huang et al*., 2012], so we include this region in the southern Africa domain.

3.1. Biomass Burning Regime

[13] Figure 2 shows the seasonal aerosol vertical profile of the extinction coefficient for the biomass burning regime areas. In South America, the aerosol extinction profile generally shows a monotonically decreasing pattern from the surface to the upper level during all seasons, except austral winter (JJA) and spring (SON) seasons. The maximum extinction occurs near the surface in SON, which corresponds to the strongest biomass burning during this period [*Dwyer et al*., 2000; *van der Werf et al*., 2003; *Huang et al*., 2012]. Since biomass burning aerosol is the dominant aerosol in this region, dust extinction is much less than all-aerosol extinction at all levels. In southern Africa, the all-aerosol extinction profile shows two peaks during austral winter and spring, at ~500 m and 3 km. The lower peak is probably due to the strong biomass burning during the dry seasons [*Dwyer et al*., 2000]. During austral fall and winter, dust extinction appears much closer to all-aerosol extinction above 4 km than lower levels, suggesting the larger impact of dust in the upper levels. In SE Asia, the aerosol extinction profile does not show much seasonal variation, possibly due to the little seasonal variation of fire emissions in this region [*Duncan et al*., 2003]. Moreover, only one peak occurs near the surface (~500 m) during all seasons, which is different from southern Africa. Similar to South America, dust contributes little to the all-aerosol extinction.

[14] To characterize the occurrence frequency distribution of different aerosol types, we calculate each aerosol type occurrence frequency by dividing the number of aerosol type samples by the total number of CALIPSO measurements (including both clear air and aerosol) within each vertical layer. The total numbers of aerosol samples (after data screening) detected by CALIPSO at each layer are shown in the Appendix (Figures A1–A4). Generally, CALIPSO detects more aerosol samples during nighttime than daytime, especially in the middle to upper troposphere, and there are fewer aerosol samples detected at high altitudes. Figure 3 shows the vertical profile of each aerosol type occurrence frequency during each season. In South America, smoke is the dominant aerosol type detected at 2–8 km during all seasons. During the strongest biomass burning season (SON), it is also the dominant type detected near the surface (~1 km). Polluted dust, which is intended to represent a mixture of smoke and dust [*Omar et al*., 2009], is the dominant aerosol detected at 1–2 km except SON when polluted continental aerosol dominates. The altitude of smoke occurrence frequency larger than 0.1% is highest in SON, at ~9 km.

[15] In southern Africa, aerosol occurrence frequency has large seasonal variations. Smoke dominates above 6 km in nearly all seasons. In MAM, dust is the dominant aerosol detected from 1 to 6 km, while polluted dust is the secondary dominant type. In JJA, dust only prevails from 4 to 7 km, and smoke prevails from 1 to 4 km. In SON, smoke becomes the dominant aerosol detected from ~2.5 km to the upper troposphere (~11 km), consistent with the strongest biomass burning during this period. Dust aerosol occurrence is lowest compared to other seasons. In DJF, polluted dust appears as the most prevailing aerosol type detected from near the surface to 6 km, while dust is the secondary type. The complexity of seasonal aerosol type variation reflects the significant impacts of both biomass burning and desert on the

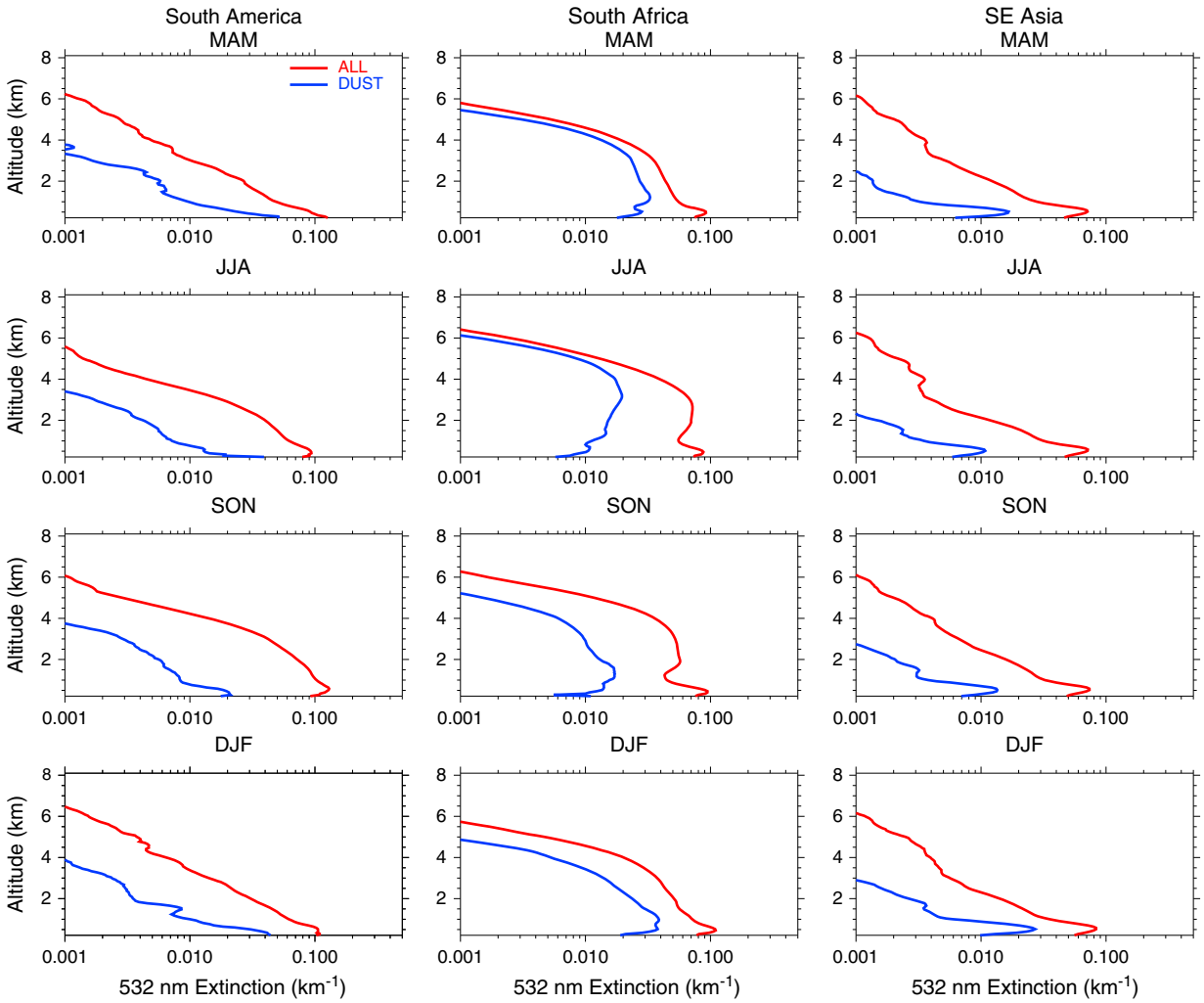

Figure 2. Profiles of the seasonal average aerosol extinction coefficient (km^{-1}) from 5-year CALIPSO observations over (left) South America, (middle) southern Africa, and (right) Southeast Asia. From top to bottom are seasonal averages for boreal spring (MAM), summer (JJA), fall (SON), and winter (DJF), respectively. The red curve represents all-aerosols (regardless of type), and the blue curve represents dust aerosol only.

aerosol composition in this region. In SE Asia, aerosol types show little seasonal variation. Throughout the year, smoke is the dominant type detected above 4 km, with a frequency peak of ~0.03 around 4 km in SON. Clean marine aerosol appears to be the dominant type detected below 4 km, due to a large oceanic area in this domain. Polluted dust is the secondary type at nearly all levels, but its occurrence frequency is comparable with that of clean marine and smoke detected around 4 km.

[16] To further characterize the vertical distribution of the aerosol layer, we also analyzed the occurrence frequency of the maximum aerosol layer top altitudes detected by CALIPSO. The Level 3 aerosol data provide the distributions of the highest aerosol layer top altitudes detected within each latitude/longitude grid cell, which are stored in 11-element percentile arrays with the first value containing the minimum layer top altitude and the last containing the maximum [*CALIPSO*, 2011]. The occurrence frequency of the maximum aerosol layer top altitude in the *i*th 500 m vertical bin (f_i) is calculated as $f_i = \frac{N_i}{\sum_{i=0}^{n} N_i}$. N_i is the number of times when the maximum aerosol layer top altitude detected by CALIPSO falls in the *i*th 500 m vertical bin, n is the total number of 500 m vertical bins. The results are shown in Figure 4. In South America, the altitude of the peak occurrence frequency of the dust aerosol layer top is significantly lower than that of all-aerosol in nearly all seasons. The altitude of the peak occurrence frequency of the dust layer top is ~3 km throughout the year, while that for all-aerosol can be as high as 7 km during wet seasons (DJF and MAM). In southern Africa, the altitude of the peak occurrence frequency of the dust layer top is much closer to that of all-aerosol in MAM and JJA than in other seasons, possibly due to the dominant role of dust in the upper level aerosol composition. The dust layer top altitude has two frequency peaks in JJA, with the peak at ~5 km close to the solitary peak of all-aerosol and larger than the

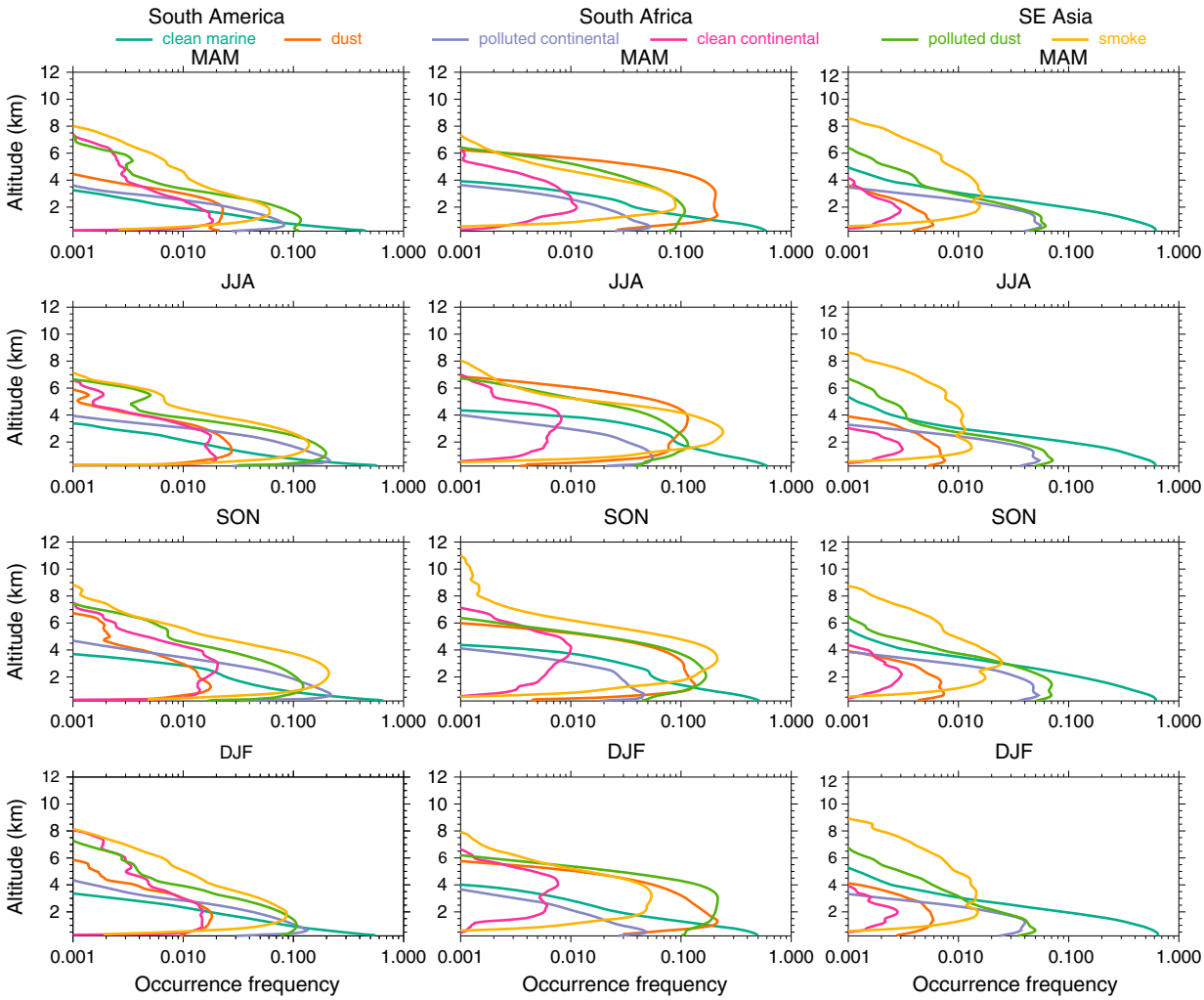

Figure 3. Seasonal occurrence frequency profile of each aerosol type from 5-year CALIPSO observations over (left) South America, (middle) southern Africa, and (right) Southeast Asia. From top to bottom are seasonal statistics for boreal spring (MAM), summer (JJA), fall (SON), and winter (DJF), respectively. The different colors represent the different aerosol types, i.e., clean marine (light green), dust (dark orange), polluted continental (slate blue), clean continental (magenta), polluted dust (green), and smoke (orange).

peak at ~1 km, suggesting that dust is detected more at a higher level than near the surface. In SE Asia, the occurrence frequency of the aerosol layer top altitude shows little seasonal variation, with a peak altitude at ~7 km for all-aerosol and ~1–2 km for dust. Dust appears to be mostly restrained in the boundary layer.

[17] In general, over biomass burning regime areas, smoke is the dominant aerosol type detected from the lower to middle troposphere. Dust contributes little to the all-aerosol extinction from the surface to the lower troposphere and has a lower altitude of peak occurrence frequency than all-aerosol. However, due to different geographic location and meteorological conditions, each region also has its unique features. In South America, the altitude of the peak occurrence frequency of the all-aerosol layer top is higher during wet seasons than dry seasons (JJA and SON). In southern Africa, dust is a significant component of the aerosols during MAM and JJA, especially in the upper level. In SE Asia, both aerosol extinction and types show little seasonal variations, partly due to the little seasonal variation of aerosol emissions.

3.2. Desert Regime

[18] The Sahara, Arabian, Gobi, and Taklamakan deserts are among the largest deserts in the world: the former two are included in the northern Africa domain, and the latter two are included in the west China domain. The Great Victoria and Great Sandy deserts are the two largest deserts in Australia and are included in the west Australia domain. The seasonal vertical profiles of aerosol extinction for these desert regime areas are shown in Figure 5. In northern Africa, the dust extinction profile is highly overlapped with the all-aerosol extinction profile, especially during MAM and JJA, suggesting the overwhelming role of dust in the

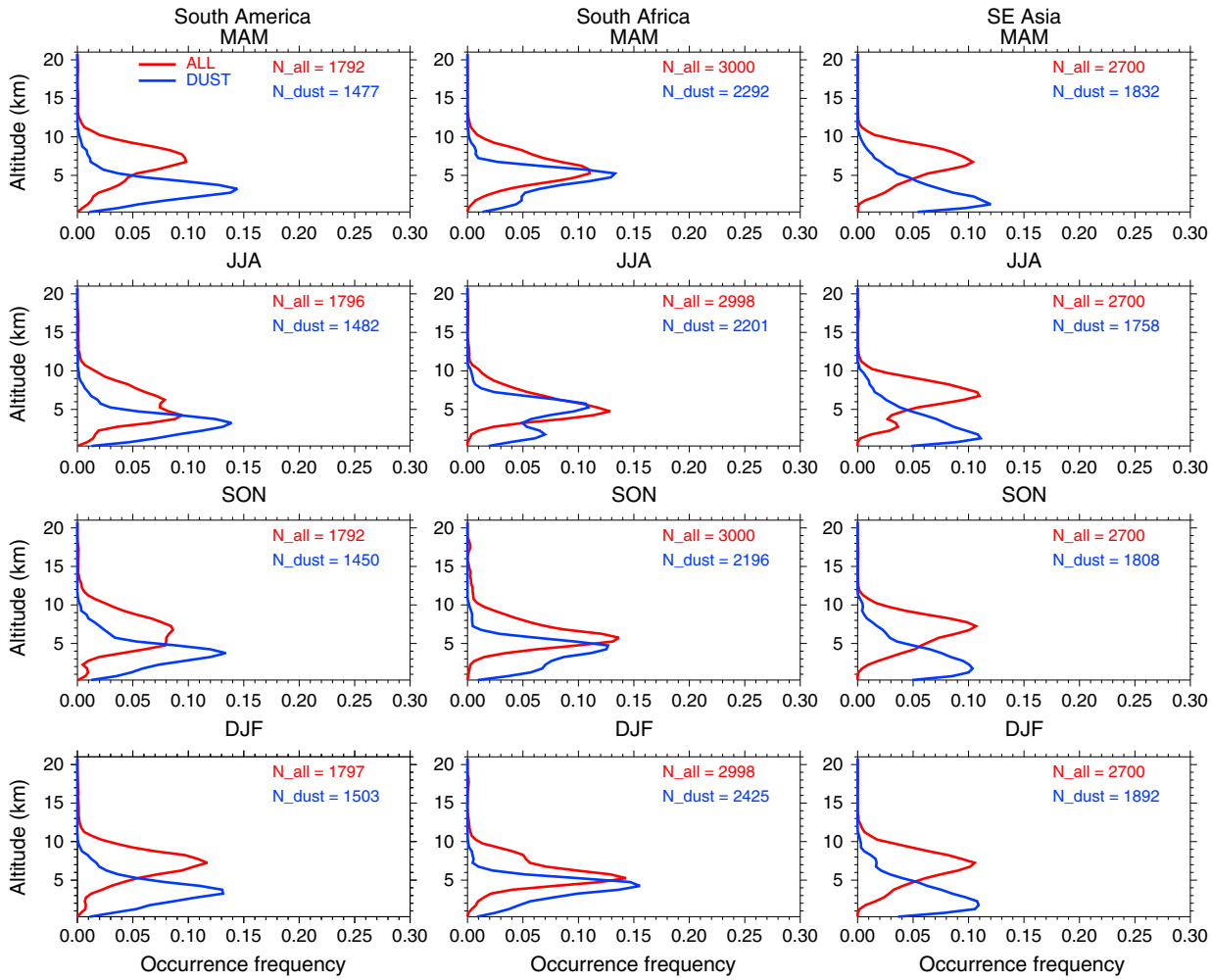

Figure 4. Seasonal occurrence frequency of maximum aerosol layer top altitudes from 5-year CALIPSO observations over (left) South America, (middle) southern Africa, and (right) Southeast Asia. From top to bottom are seasonal statistics for boreal spring (MAM), summer (JJA), fall (SON), and winter (DJF), respectively. The red curve represents all-aerosols (regardless of type) that are included in the statistics, and the blue curve represents dust aerosol only. The numbers in each panel indicate the total number of samples for all-aerosols (red) and dust aerosol only (blue).

aerosol composition over this region. During DJF, the dust contribution to all-aerosol extinction is weaker than other seasons, particularly above 2 km, and the extinction decreases more rapidly with altitude. The maximum altitude of the dust extinction greater than 0.001 km^{-1} is ~7 km in JJA, ~6 km in MAM and SON and ~4.5 km in DJF. The largest extinction near the surface occurs in JJA (greater than 0.2 km^{-1}). In west China, the overlap only occurs in MAM, corresponding to the annual heavy dust storm during boreal spring season [e.g., *Husar et al*., 2001]. Moreover, aerosol extinction reaches the largest value near the surface (greater than 0.3 km^{-1}) also in MAM. Although aerosol extinction is largest at the surface and decreases with altitude, there is a secondary peak around ~2.5 km during MAM and JJA. Aerosol extinction decreases more rapidly with altitude during DJF than other seasons. The maximum altitude of aerosol extinction greater than 0.001 km^{-1} is ~7.5 km in MAM and JJA and ~6–6.5 km in SON and DJF.

[19] In west Australia, the pattern is totally different from the former two regions. The dust extinction profile is far away from the all-aerosol extinction profile, suggesting dust contributes little to the all-aerosol extinction. The low dust output may be partly explained by the fact that the continent has relatively low topographical relief, and the arid regions are old and highly weathered, i.e., fine particles were blown away a long time ago [*Prospero et al*., 2002]. Both dust and all-aerosol extinction decrease monotonically with altitude. The maximum extinction of dust near the surface is less than 0.01 km^{-1}. During MAM and JJA, the maximum altitude of aerosol extinction greater than 0.001 km^{-1} is ~1–1.5 km lower than that during SON and DJF.

[20] Regarding the aerosol type distribution (Figure 6), the three domains have quite distinct features. In northern Africa, dust is the dominant aerosol type with an occurrence frequency more than 50% and nearly constant detected from ~1 to ~4 km during all seasons except DJF, and polluted dust is the secondary type. Above 4 km, the dust occurrence

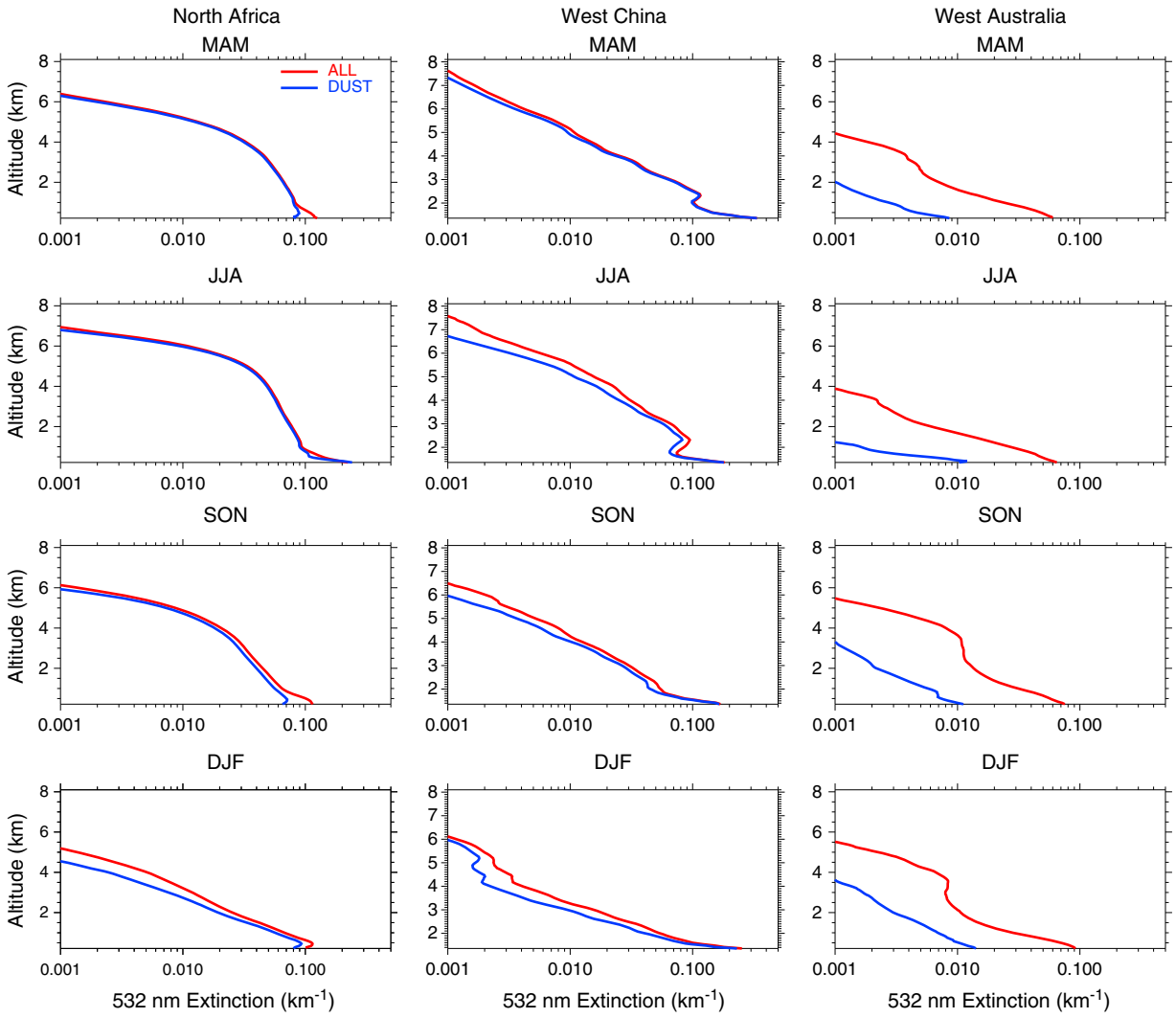

Figure 5. Same as Figure 2 but over (left) northern Africa, (middle) west China, and (right) west Australia.

frequency decreases rapidly with altitude. The maximum altitude of the dust occurrence frequency larger than 0.1% is 10 km in MAM, 9 km in JJA, and 7 km in SON and DJF. Both dust and polluted dust are dominant types above 4 km in DJF. The occurrence frequency of other aerosol types is negligible compared with the former two types (the large frequency of clean marine aerosol near 0 m amsl occurs over the small oceanic regions in the NAF domain; see Figure 1). In west China, the dust occurrence frequency peaks near the surface and decreases rapidly with altitude in all seasons except MAM. During MAM, the dust occurrence frequency is still larger than 2% and 0.1% detected at 8 and 11 km, respectively. Similar to northern Africa, polluted dust is the secondary type, with the occurrence frequency comparable to dust in the upper level. Although smoke is the third dominant type, its occurrence frequency is about 1 order of magnitude less than polluted dust. In west Australia, polluted dust is the dominant type detected from ~1 to ~5 km, and smoke dominates above 5 km in all seasons except JJA. During JJA, smoke becomes the dominant type above 3 km. The maximum occurrence frequency of dust is less than 5% in MAM and JJA and ~10% near the surface in SON and DJF. To some extent, the aerosol type occurrence frequency over this region is similar to some biomass burning areas (e.g., South America).

[21] Figure 7 shows the occurrence frequency of the maximum aerosol layer top altitudes. In northern Africa, the frequency profiles of dust and all-aerosol are closely overlapped in MAM and JJA, again suggesting the dominant role of dust. The altitude of the peak frequency is significantly higher in MAM and JJA than the other two seasons. A remarkable feature is that a secondary all-aerosol frequency peak (greater than 2%) occurs at ~18 km only during JJA. This peak suggests that an aerosol layer may exist at the tropopause level, which is presumably associated with the Asian tropopause aerosol layer as first discovered by *Vernier et al*. [2011]. In west China, during the strong dust storm season (MAM), the frequency profile of dust overlaps with that of all-aerosol. During other seasons, the altitude of the dust peak frequency is slightly lower than that of all-aerosol.

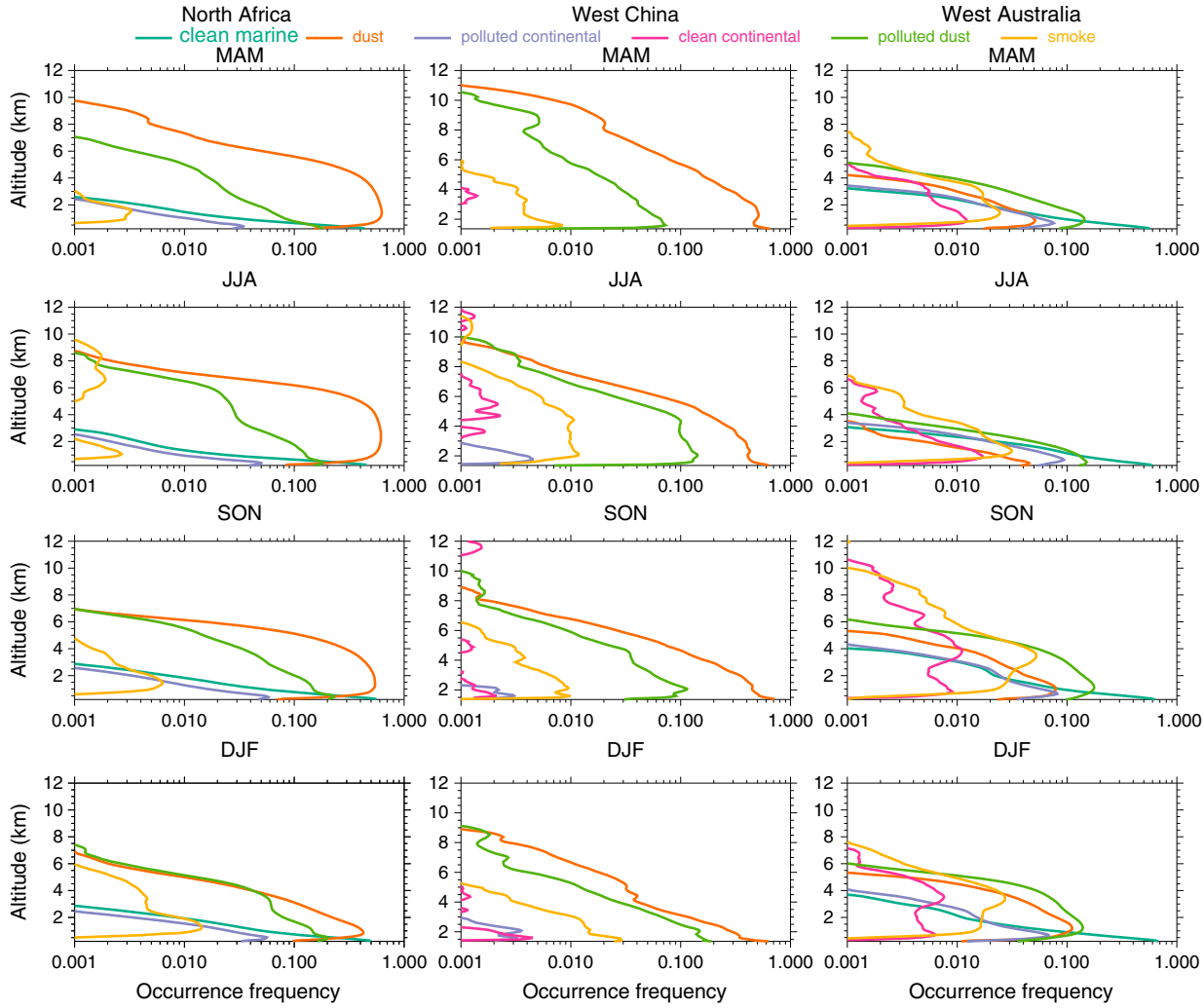

Figure 6. Same as Figure 3 but over (left) northern Africa, (middle) west China, and (right) west Australia.

Similar to northern Africa, a secondary all-aerosol frequency peak (~3%) occurs at ~18 km only during JJA. In west Australia, the dust layer occurs most frequently in the boundary layer except in DJF, consistent with the little fraction of dust in aerosol composition. There are two frequency peaks of all-aerosol during MAM and JJA: one at ~7 km and the other at ~4 km. During SON and DJF, the peak frequency of all-aerosol occurs at ~5 km.

[22] In general, over desert regime areas, dust is the dominant aerosol type from the surface to the middle troposphere and sometimes can extend to above 8 km. Dust contributes significantly to the all-aerosol extinction and has nearly the same layer top altitude of the peak occurrence frequency as all-aerosol. However, west Australia is an exception. Despite the desert and arid surface type, the aerosol characteristics in this region are closer to the biomass burning regime rather than the desert regime. This is mainly due to two reasons: first, the continent has relatively low topographical relief, and the arid regions are old and highly weathered [*Prospero et al.*, 2002]; second, both northern and western regions of Australia have active fire seasons [*Giglio et al.*, 2006], with substantial emissions of biomass burning generated aerosol. A notable common feature in northern Africa and west China is a secondary peak (2%–3%) of the layer top occurrence frequency of all-aerosol at ~18 km only during JJA, suggesting the existence of an aerosol layer at the tropopause level during boreal summer.

3.3. Fossil Fuel and Industry Regime

[23] In India, east China, west Europe, and East U.S., fossil fuel, biofuel burning, and industry generated aerosols are a major part of the total aerosol loading [*Duncan et al.*, 2007]. Figure 8 shows the seasonal vertical profiles of aerosol extinction for these four domains. In India, the extinction profile of dust is close to that of all-aerosol in MAM and JJA, suggesting the significant contribution of dust which is presumably transported from the nearby Thar and Arabian deserts. Moreover, dust with extinction greater than 0.001 km^{-1} can reach as high as 6 km, about 1.5–2.5 km higher than that in SON and DJF. The maximum extinction occurs

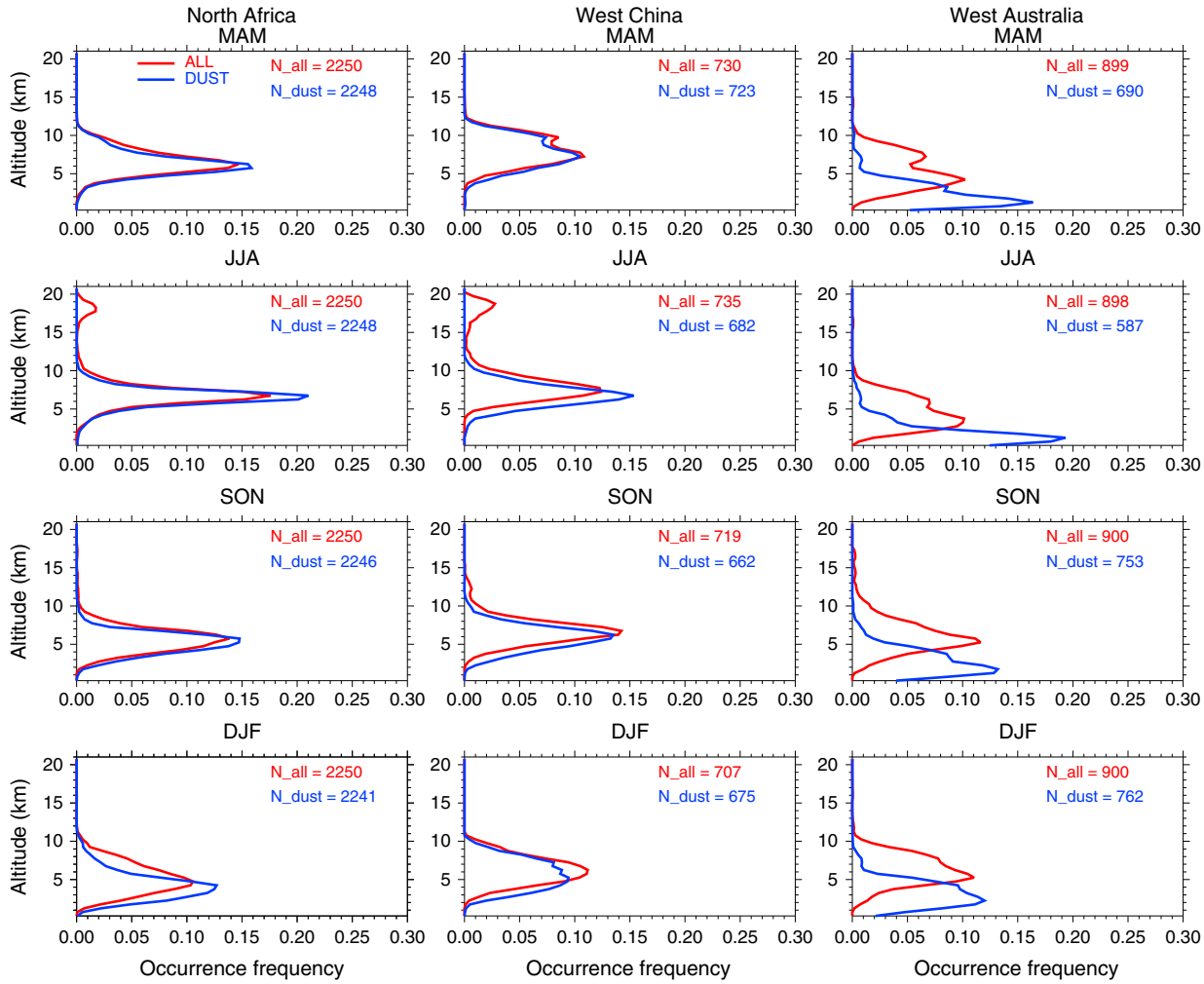

Figure 7. Same as Figure 4 but over (left) northern Africa, (middle) west China, and (right) west Australia.

at the surface and decreases with altitude. During JJA, surface aerosol extinction is close to 0.5 km^{-1}, ~2–3 times larger than during other seasons. During SON and DJF, aerosol extinction decreases more rapidly with altitude than during MAM and JJA, and the maximum extinction occurs slightly above the surface. In east China, dust contribution is much weaker than in India. During MAM, the dust extinction profile is closer to the all-aerosol extinction profile than during other seasons, due to the strong transport of dust from west China. The shape of the all-aerosol extinction profile does not change much throughout the year, but the maximum altitude of extinction greater than 0.001 km^{-1} has seasonal change, with the highest altitude at ~7 km in MAM. In west Europe, dust appears to contribute more to all-aerosol extinction in the upper level than the lower level, especially in MAM and JJA. The maximum altitude of all-aerosol extinction greater than 0.001 km^{-1} is highest in JJA (~6 km) and lowest in DJF (~4.5 km). In East U.S., the dust extinction profile is far away from the all-aerosol extinction profile and decreases rapidly with altitude. This is not surprising since no big desert is included in this domain or nearby. The maximum altitude of all-aerosol extinction greater than 0.001 km^{-1} is about 1.5 km higher in MAM and JJA than in other seasons.

[24] The seasonal vertical profile of each aerosol type occurrence frequency is shown in Figure 9. In India, dust dominates from near the surface to as high as 10 km in MAM, and polluted dust is the secondary type; other aerosol types are trivial. In JJA and SON, the type distribution is complicated because dust, polluted dust, and smoke all play important roles. For example, in SON, polluted dust, dust, and smoke dominate at 1–3, 3–5.5, and 5.5–8 km, respectively. However, smoke always dominates at higher levels than dust. In DJF, all-aerosol types are limited below 6 km. In east China, dust dominates above 2 and 3 km in MAM and DJF, respectively, while polluted dust dominates in the lower level. Dust with an occurrence frequency larger than 0.1% can reach as high as 11 km during MAM. In JJA and SON, similar to India, all three types are important. However, dust dominates at higher levels than smoke, which is different from India. In west Europe, dust dominates above 3 km in all seasons except DJF, but the maximum altitude has seasonal change. The higher occurrence frequency of smoke above 8 km in JJA and SON may be artificial due to

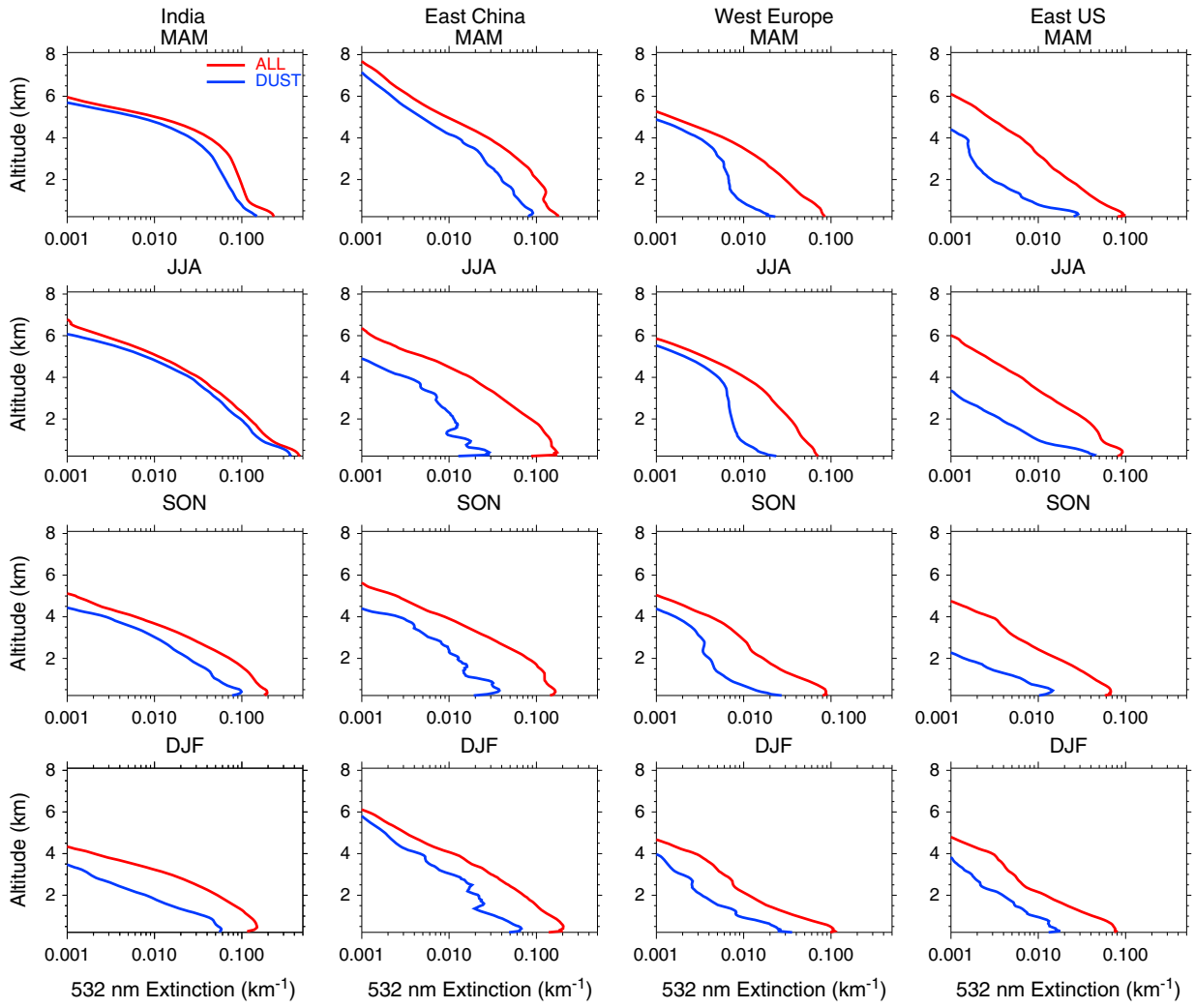

Figure 8. Same as Figure 2 but over (left) India, (second column from left) east China, (third column from left) west Europe, and (right) East U.S.

misclassification. Polluted dust dominates below 3 km in all seasons except DJF. Aerosols are classified as smoke less often than dust and polluted dust in this region. This could be caused by smoke and dust mixing in the lower troposphere and being classified as polluted dust or could be because smoke does not contribute significantly to total aerosol loading. During DJF, the aerosol occurrence frequency is much less than during other seasons and mostly limited below 6 km. In East U.S., aerosol classified as polluted dust dominates in the lower to middle troposphere and up to 6 km. However, polluted dust can reach as high as 10 km in MAM and JJA. Smoke prevails above 5 km during JJA and SON. Dust is detected as the dominant type at 6–8 and 5–7 km over this region during MAM and DJF, respectively.

[25] As for the occurrence frequency of the maximum aerosol layer top altitudes, the four regions have similar patterns (Figure 10). Generally, the altitude of the dust frequency peak is lower than that of all- aerosol. However, there are some exceptions. During MAM in both India and east China, the altitudes of the peak occurrence frequency for dust and all-aerosol are closely overlapped, due to the overwhelming dust in the aerosol loading. During MAM and JJA in west Europe, the altitudes of the frequency peak for the two types are also nearly the same, which may be due to the more significant impact of dust in the upper level than the lower level, as shown by the extinction profiles (Figure 8). Similar to northern Africa and west China, a secondary occurrence frequency peak (2%) of all-aerosol occurs at ~18 km only during JJA over India and east China, again suggesting the existence of a tropopause aerosol layer only during this season.

[26] In general, over fossil fuel and industry regime areas, the dominant aerosol types include polluted dust, smoke, and dust, with each type dominating at different levels. The dominant aerosol types also have large geographical and seasonal variations. Dust contribution to the all-aerosol extinction is highly dependent on the location and season. If big desert areas are included in the domain or nearby, dust can play an important role during some specific periods (e.g., MAM in India and east China). During other periods, dust has little impact on the all-aerosol extinction and has

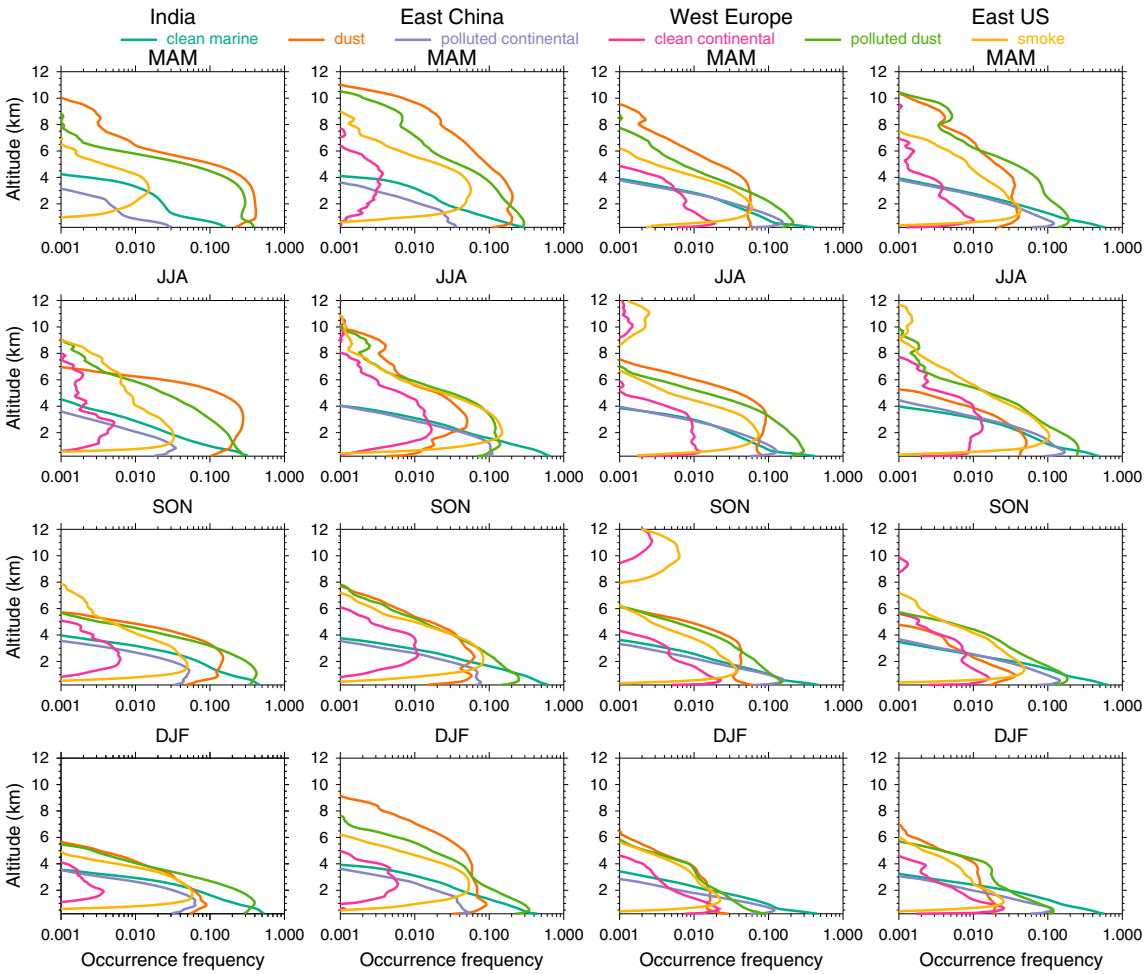

Figure 9. Same as Figure 3 but over (left) India, (second column from left) east China, (third column from left) west Europe, and (right) East U.S.

lower altitude of the peak occurrence frequency than all aerosol. A notable common feature again shows up in India and east China, i.e., a distinct secondary layer top frequency peak of all-aerosol occurs at ~18 km only during JJA (Figure 10).

3.4. Oceanic Regime

[27] Oceans serve as a significant source of gaseous and aerosol emissions, due to their coverage of more than two thirds of the Earth surface. The emissions from oceans could mix with ship and continental emissions and form a complicated mixture of marine aerosol particles. Thus, the sources and properties of marine aerosols can be affected by ocean emissions, ship exhaust, and transported continental emissions [*Sorooshian and Duong*, 2010]. Here we choose three oceanic regions, and their seasonal vertical profiles of aerosol extinction are shown in Figure 11. Over NW Pacific, dust contributes little to the all-aerosol extinction throughout the year. However, dust still has some impact on the boundary layer during JJA, with dust extinction decreasing rapidly with altitude. The maximum altitude of extinction greater than 0.001 km^{-1} is highest in MAM, ~6 km for dust, and ~8 km for all-aerosol. This is consistent with the well-known trans-Pacific transport of dust at 4–6 km during this period [e.g., *Husar et al.*, 2001; *Eguchi et al.*, 2009]. During other seasons, dust is mostly restrained in the lower troposphere and has local impact. Over North Atlantic, the seasonal pattern of all-aerosol is similar to that over NW Pacific, except that the maximum altitude of extinction greater than 0.001 km^{-1} is much lower. The maximum altitude is ~5.5 km in MAM and JJA and ~4.5 km in SON and DJF. As for dust, the maximum altitude is highest in JJA (~5 km). Dust impact is much larger over central Atlantic than over the former two regions, especially during MAM and JJA. In both seasons, the extinction profile of dust is much closer to that of all-aerosol in the upper level than the lower level, suggesting the larger impact of transported Saharan desert dust in the upper level. During other seasons, dust impact is much smaller. The maximum altitude of extinction greater than 0.001 km^{-1} is highest in JJA, ~6 km for both dust and all-aerosol.

[28] The seasonal vertical profile of each aerosol type occurrence frequency is shown in Figure 12. Over NW Pacific, clean marine is the dominant type from the surface up to 3 km in nearly all seasons. Polluted dust dominates from ~1 to 4 km, and both dust and polluted dust are

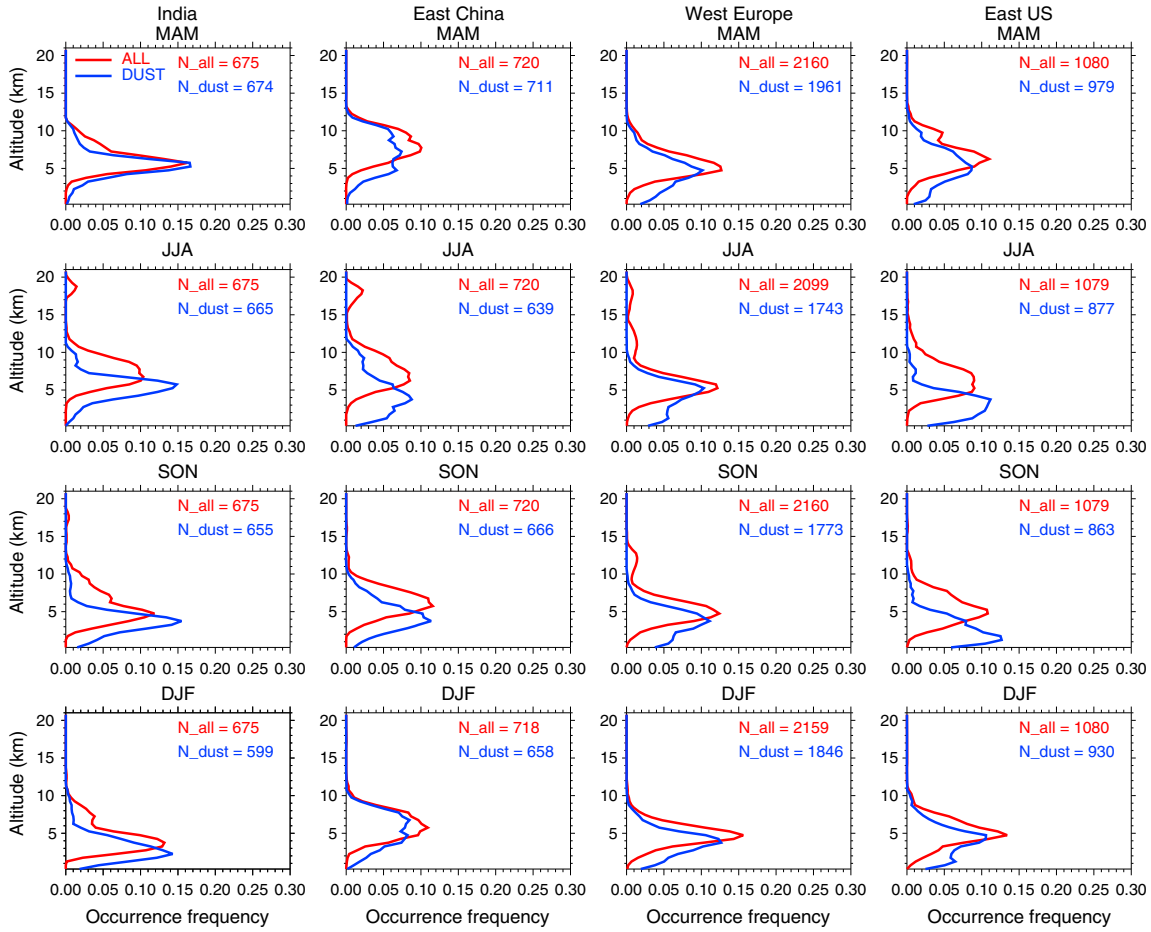

Figure 10. Same as Figure 4 but over (left) India, (second column from left) east China, (third column from left) west Europe, and (right) East U.S.

dominant types at 4–10 km in MAM. Smoke plays an important role above 3 km in JJA and SON, although polluted dust has a comparable frequency below 8 km. The relatively high occurrence frequency of smoke in the middle to upper troposphere could be due to transport of fire generated aerosols in Eurasia during April–September across the NW Pacific [e.g., *Dwyer et al.*, 2000; *Damoah et al.*, 2004]. During DJF, dust becomes important again, dominating from 5 to 9 km. Over North Atlantic, dust is the dominant type at 2.5–4.5 km during JJA and SON, while smoke dominates above 4.5 km. In MAM, dust and polluted dust are the dominant types and have comparable occurrence frequencies detected above 3 km; while in DJF, smoke becomes the dominant type above 3 km. Over central Atlantic, dust is the dominant type only in MAM and JJA at 2–6 km, consistent with its large impact on the all-aerosol extinction. Smoke always dominates above 6 km in all seasons, and its dominance can extend downward to 3 km in SON. Polluted dust is the dominant type detected at 2–5 km in DJF but is classified less often in other seasons.

[29] Regarding the occurrence frequency of the maximum aerosol layer top altitude, the three oceanic regions have similar patterns (Figure 13). The altitude of the dust frequency peak is lower than that of all-aerosol throughout the year. However, exceptions appear in DJF over NW Pacific and in MAM/JJA over central Atlantic. The altitudes of the frequency peak for dust and all-aerosol are nearly the same in these exceptional cases, presumably due to the dominant role of dust in the aerosol loading, as shown in Figure 12. Over NW Pacific, the altitudes of the frequency peak for dust and all-aerosol are highest in MAM, above 5 km. This is consistent with the extinction profile shown in Figure 11. During other seasons, the dust layer appears to be limited within the boundary layer and the lower troposphere.

[30] In general, over oceanic regime areas, the dominant aerosol types include clean marine, dust, polluted dust, and smoke; clean marine is the dominant type near the ocean surface, while the other three types have large geographical and seasonal variations, as discussed in the context above. The dust contribution to the all-aerosol extinction is small or only limited to the upper level. The dust layer top has a lower altitude of peak occurrence frequency than that of all-aerosol. Two exceptions are NW Pacific in MAM and central Atlantic in MAM/JJA. The former is related to the strong trans-Pacific transport of dust in the middle to upper troposphere from Asia, and the latter is associated with the dust output from the nearby Sahara desert.

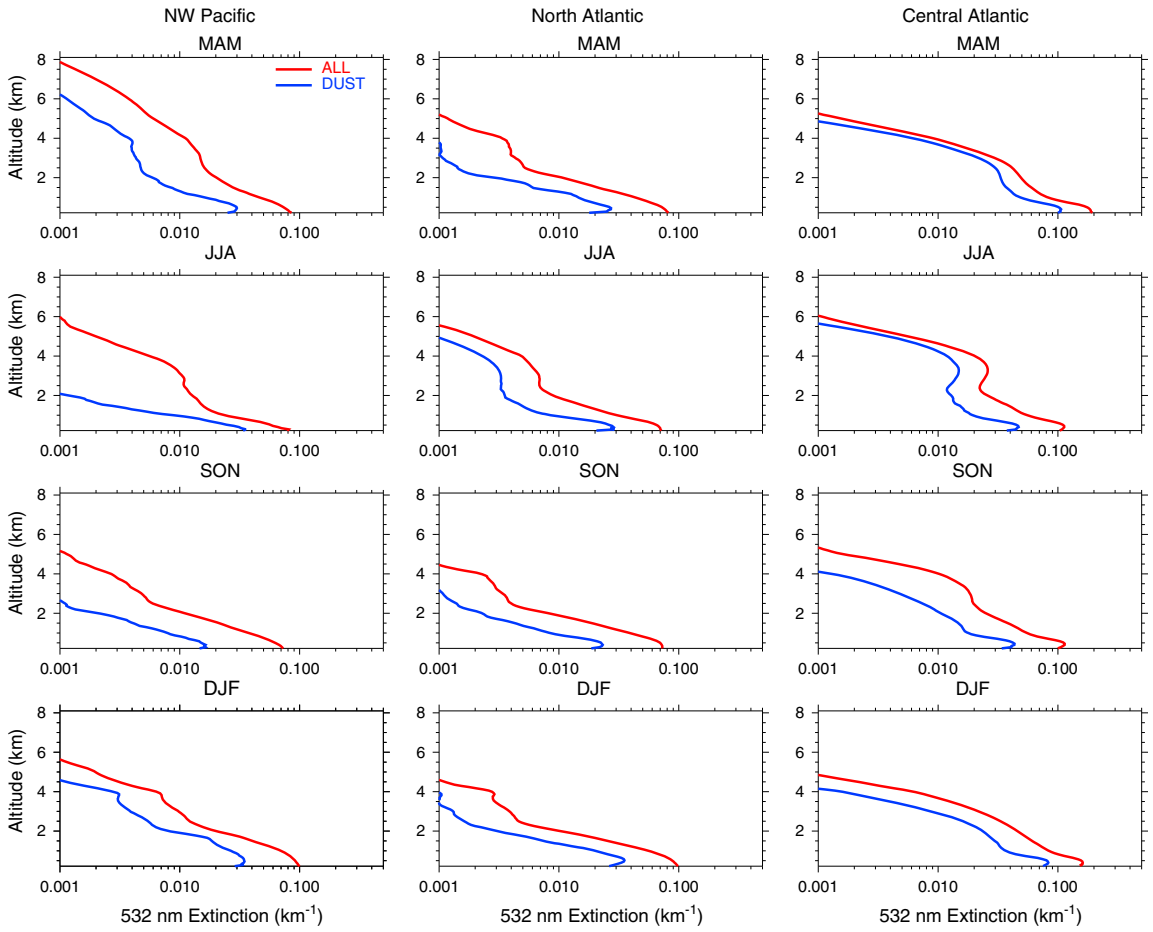

Figure 11. Same as Figure 2 but over (left) northwest Pacific, (middle) North Atlantic, and (right) central Atlantic.

4. Diurnal Variation of the Vertical Distribution of Aerosol Properties

[31] The CALIPSO measurements are divided into daytime and nighttime periods, providing an opportunity for us to evaluate aerosol diurnal variability. However, it is important to recognize that two phenomena are observed by CALIPSO Level 3 data, namely, natural diurnal variability and artificial diurnal variability due to differences in layer detection and type classification at daytime relative to nighttime. The CALIPSO signal is noisier during daytime, causing some optically thin layers to go undetected that would have otherwise been detected at nighttime. Aerosol typing is also affected because depolarization, a ratio of two noisy numbers, is used to discriminate between aerosol types. Increased noise may generate a different aerosol type classification during daytime than if the layer was classified at nighttime. Since there is a statistical difference in daytime versus nighttime layer detection sensitivity, Level 3 averaging tends to elucidate artificial diurnal variability. In the discussion that follows, observations that are possibly related to natural diurnal variability are noted, although artificial diurnal variability could also play a role. More work is needed in the future to determine the relative importance of these two diurnal variabilities.

[32] We have analyzed the differences of aerosol extinction, occurrence frequency of aerosol type, and layer top altitude between daytime and nighttime, and the results show little seasonal variation. Thus, in the following discussion, we only choose JJA season to illustrate the diurnal variation of detected aerosol properties. The differences are calculated as nighttime minus daytime measurements.

[33] *Biomass burning regime* (Figure 14). The positive values of the all-aerosol extinction difference suggest larger extinction during nighttime. However, the altitude of the difference peak is dependent on the region. In South America, the difference peaks near the surface and decreases with altitude. In southern Africa, the difference peaks at ~3 km. In SE Asia, the difference peaks at ~1.5 km and changes sign below 1 km. Dust extinction shows a much smaller diurnal difference compared with all-aerosol. Generally, smoke and polluted continental aerosols are detected more frequently during nighttime in the lower troposphere, while polluted dust is detected less frequently below 1 km. In South America, polluted dust has a higher occurrence frequency detected at 1–3 km during nighttime. In southern Africa and SE Asia, clean marine aerosol is detected more frequently from the surface to ~4 km during nighttime. Regarding the occurrence frequency of the maximum aerosol layer top altitude, during

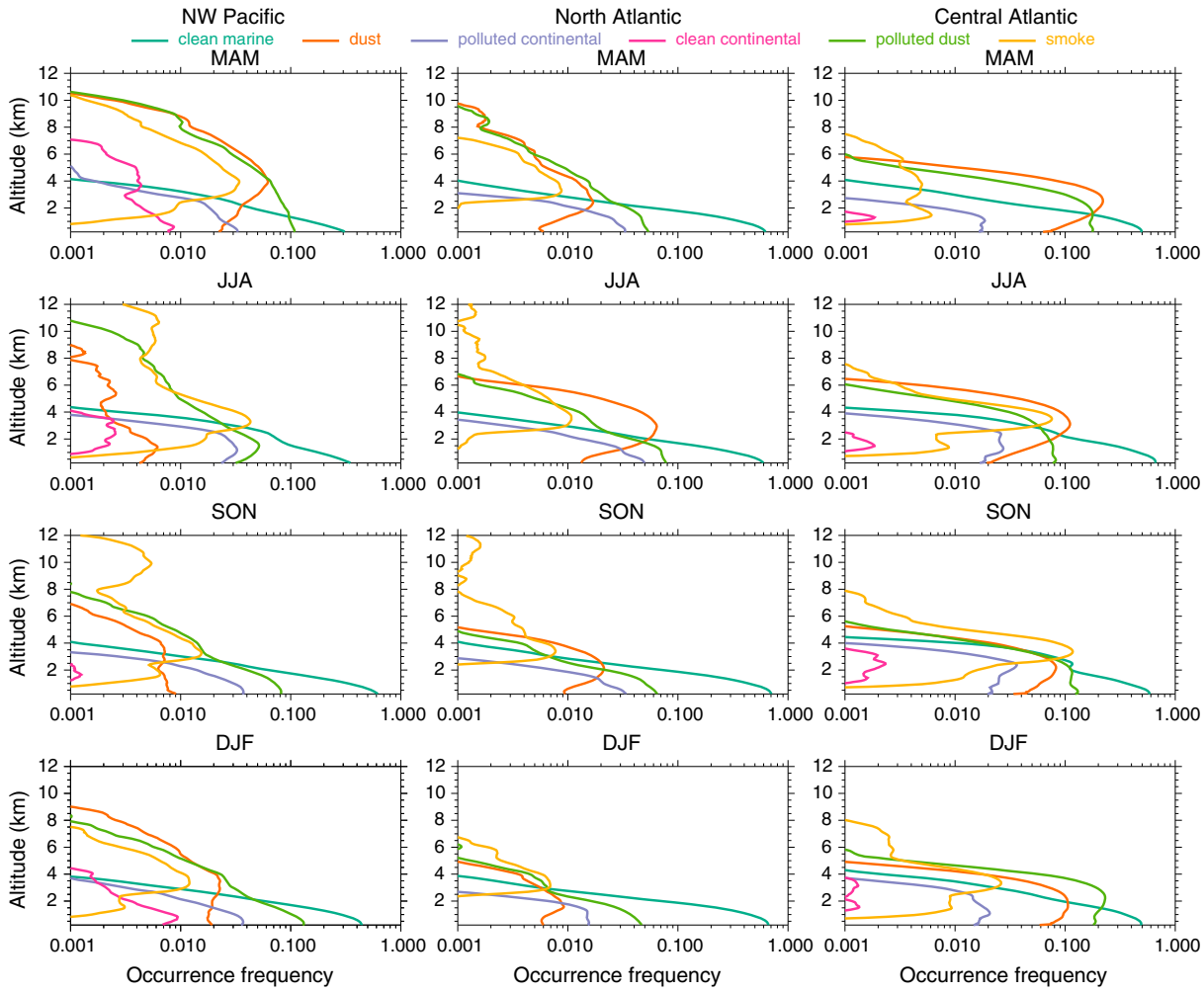

Figure 12. Same as Figure 3 but over (left) northwest Pacific, (middle) North Atlantic, and (right) central Atlantic.

nighttime, the aerosol layer top is observed at high altitudes more frequently than during daytime. Both dust and all-aerosol show this diurnal variation, although dust variability is much smaller than that of all-aerosol. One exception is in southern Africa, where the dust layer top also shows a higher occurrence frequency in the boundary layer and dust variability is comparable to that of all-aerosol. The higher occurrence frequency of the aerosol layer top at high altitudes during nighttime may be due to two reasons: first and also the main reason, sunlight adds noise to the lidar signal, reducing the layer detection sensitivity at daytime; CALIPSO lidar has a better SNR and higher feature detection sensitivity at nighttime than daytime [*Liu et al.*, 2009b], so CALIPSO could detect more aerosols at high altitudes. Second, CALIPSO flies in a Sun-synchronous orbit, with 01:30 and 13:30 local time for crossing the equator; thus, the measurements are in the early afternoon and after midnight. Numerous observations have shown that over land, the diurnal maxima of deep convection and precipitation occur frequently in the late afternoon or early evening [e.g., *Dai et al.*, 1999; *Soden*, 2000; *Dai*, 2001; *Nesbitt and Zipser*, 2003]. The deep convective activity may transport aerosols to higher altitudes, which could also lead to a higher occurrence frequency of aerosols at high altitudes detected by CALIPSO during nighttime than daytime.

[34] *Desert regime* (Figure 15). One distinct feature is that the diurnal extinction difference profiles of dust and all aerosol are overlapped except in west Australia. This is due to the dominant role of dust in the aerosol composition. Aerosol extinction is slightly larger near the surface during nighttime than daytime. In west Australia, dust extinction shows little diurnal variation above the boundary layer. Aerosols are classified as dust and polluted dust more often at nearly all levels during nighttime, while other aerosol types are observed to have little diurnal variation, in northern Africa and west China. The diurnal difference of dust is detected about 2–3 times larger than that of polluted dust. In west Australia, polluted dust, polluted continental, and clean marine aerosols are detected more frequently from ~0.5 to 2.5 km during nighttime, while dust and other types are observed to have little diurnal variation. Similar to biomass burning areas, the occurrence frequency of the maximum aerosol layer top altitude is detected larger at high altitudes during nighttime. It is worthwhile to point out the

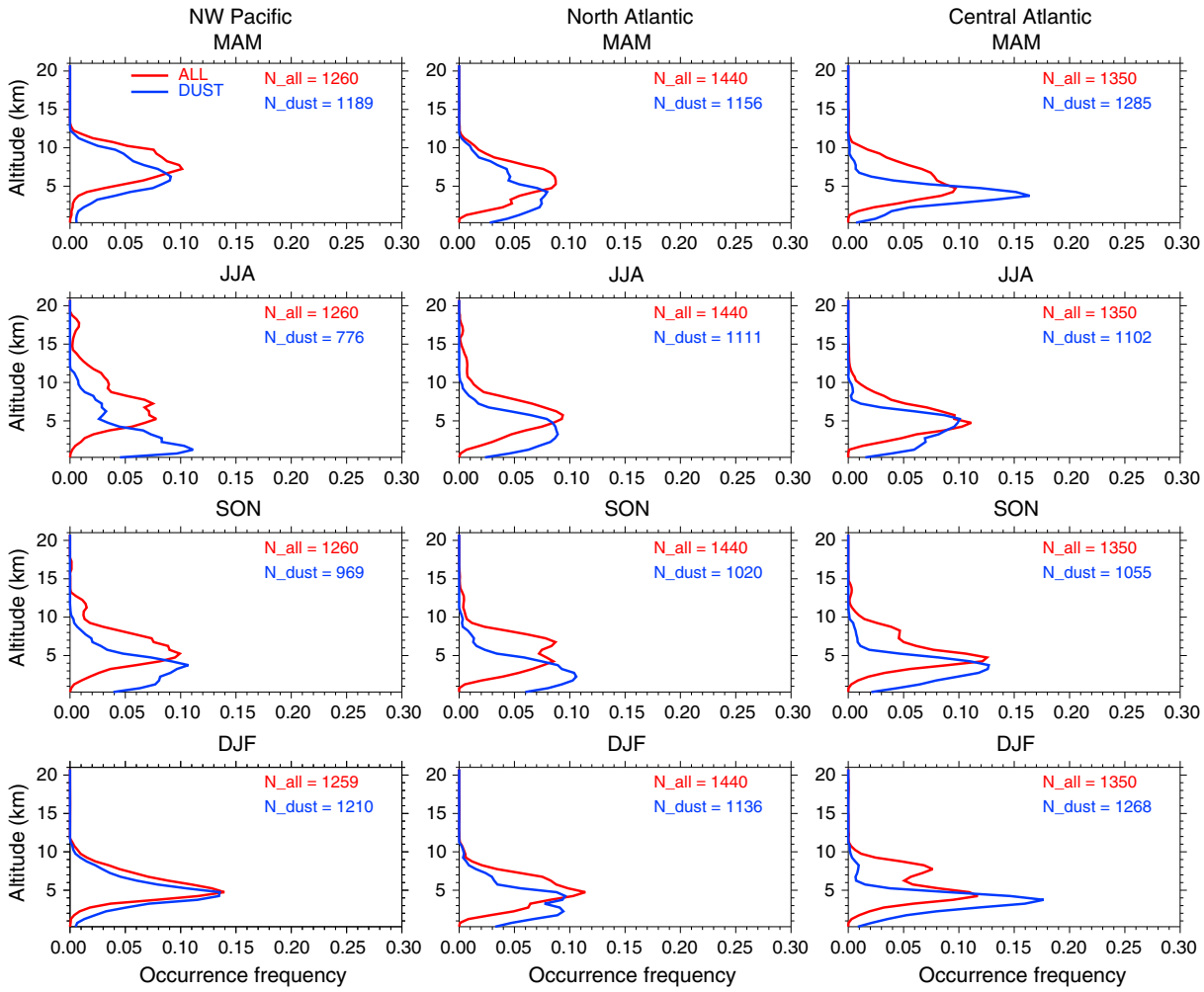

Figure 13. Same as Figure 4 but over (left) northwest Pacific, (middle) North Atlantic, and (right) central Atlantic.

positive diurnal differences of all-aerosol around 18 km in northern Africa and west China are detected only during JJA but are not detected in other seasons (not shown). This suggests that the aerosol layer which only occurs in JJA may be optically thin because it is not detected during daytime.

[35] *Fossil fuel and industry regime* (Figure 16). All-aerosol extinction is larger during nighttime at almost all levels in India and west Europe, detected at 2–6 km in East U.S. and at 1–6 km in east China. However, all-aerosol extinction is smaller during nighttime detected below 2 km in India during other seasons (not shown). Dust extinction has a much smaller diurnal variation than all-aerosol extinction, except in India and East U.S. during MAM (not shown) and JJA. The difference profile of dust extinction is closely overlapped with that of all-aerosol extinction in India, owing to the dominance of dust during MAM and JJA; during the same period, the difference of dust extinction is closely overlapped with that of all-aerosol extinction below 2 km in East U.S. As for the difference of the aerosol type occurrence frequency, smoke and polluted dust are detected more frequently during nighttime at almost all levels except in east China. However, other aerosol types have a large geographical difference. In India, dust is detected more frequently below 2 km and above 4 km and less frequently at 2–4 km during nighttime. In east China, both dust and polluted dust are detected less frequently, while polluted continental and clean marine aerosols are detected more frequently, below 2.5 km. Dust is detected more frequently at all levels during nighttime in west Europe, while it has little diurnal variation in East U.S. Similarly, the occurrence frequency of the maximum aerosol layer top altitude is larger at high altitudes during nighttime, with a larger diurnal difference of all-aerosol than dust. However, dust layers are also detected slightly more frequently within the boundary layer during nighttime. Similar to northern Africa and west China, positive diurnal differences of all-aerosol around 18 km in India and east China are only detected during JJA but are not detected in other seasons (not shown).

[36] *Oceanic regime* (Figure 17). Dust extinction is larger below 2 km at nighttime than daytime, with the maximum diurnal difference detected at the surface. This may be partly due to the effect of land-sea breeze, which is a well-known meteorological phenomenon [*Miller et al.*, 2003] caused by the temperature differences between the sea and the land near the coast. The extinction of all-aerosol is larger during nighttime at all levels over NW Pacific and above 1 km over

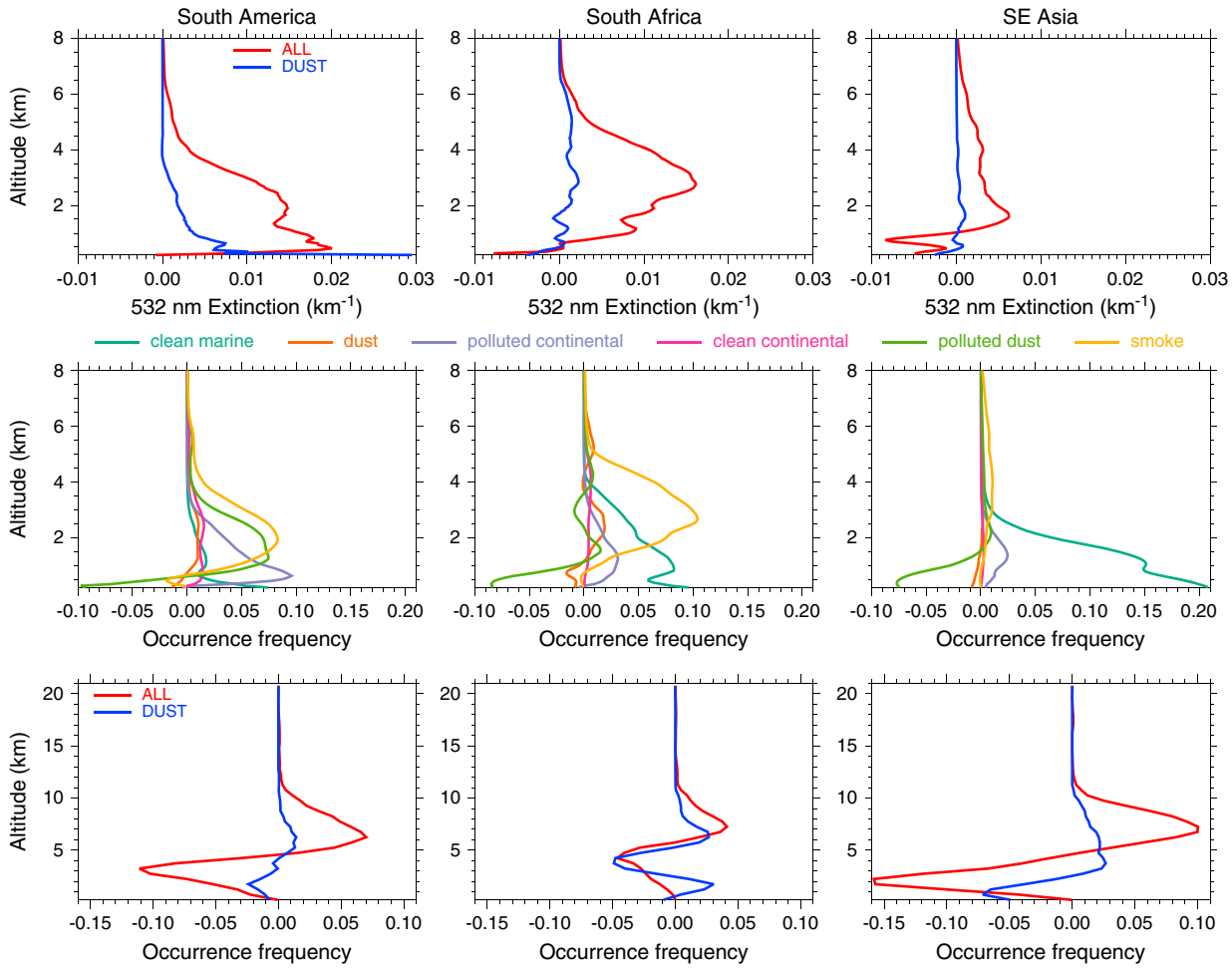

Figure 14. Diurnal variation (nighttime minus daytime measurements) of (top panel) profiles of the seasonal average aerosol extinction coefficient (km^{-1}), (middle panel) occurrence frequency profile of each aerosol type, and (bottom panel) occurrence frequency of maximum aerosol layer top altitudes, during JJA over (left) South America, (middle) southern Africa, and (right) Southeast Asia. In the top and bottom panels, the red curve represents all-aerosols (regardless of type), and the blue curve represents dust aerosol only. In the middle panel, the different colors represent the different aerosol types, i.e., clean marine (light green), dust (dark orange), polluted continental (slate blue), clean continental (magenta), polluted dust (green), and smoke (orange).

North Atlantic and central Atlantic. Polluted continental and clean marine aerosols are detected more frequently below 4 km, while polluted dust is detected less frequently below 1 km over all the oceanic regions. Over NW Pacific and central Atlantic, both polluted dust and smoke are detected more frequently above 1 km during nighttime. Over North Atlantic, smoke does not show much diurnal variation. The occurrence frequency of the maximum aerosol layer top altitude is larger at high altitudes during nighttime, with a larger diurnal difference of all-aerosol than dust. One exception is over central Atlantic, where the dust layer is also detected more frequently above the surface (2–3 km) during nighttime. Positive diurnal differences of all-aerosol around 18 km are only obvious over NW Pacific during JJA.

5. Summary and Conclusions

[37] We have performed a statistical analysis of seasonal vertical distributions of aerosol properties, including extinction coefficient, aerosol type, and maximum aerosol layer top altitude, based on CALIPSO lidar measurements at 532 nm during nighttime from March 2007 to February 2012. The diurnal variations (differences between nighttime and daytime measurements) of aerosol properties are also discussed. We selected 13 domains and categorized them into four groups according to their surface aerosol emission regimes. The regional and seasonal variations of the vertical distribution of aerosol properties are summarized in the following.

[38] *Biomass burning regime*:

[39] 1. Smoke is the dominant aerosol type detected from the lower to the middle troposphere.

[40] 2. Dust contributes little to all-aerosol extinction from the surface to the lower troposphere. The dust layer top has a lower altitude of the peak occurrence frequency than that of all-aerosol.

[41] 3. In South America, the altitude of the peak occurrence frequency of the dust layer top is 3 km throughout

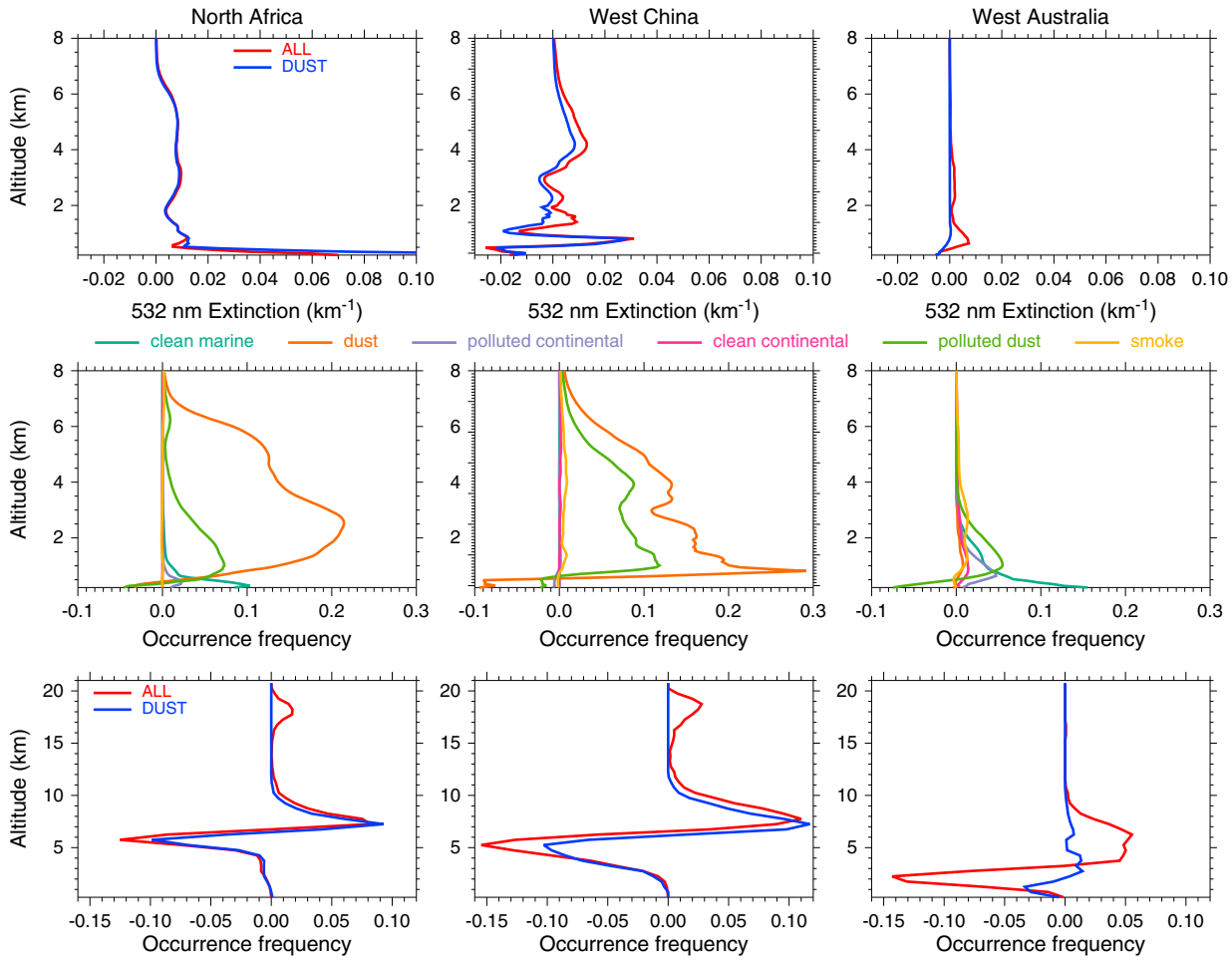

Figure 15. Same as Figure 14 but over (left) northern Africa, (middle) west China, and (right) west Australia.

the year, while that of all-aerosol can reach 7 km during wet seasons.

[42] 4. In southern Africa, the all-aerosol extinction profile shows two peaks, at ~500 and 3 km in JJA and SON. During MAM and JJA, dust has larger impact on all-aerosol extinction above 4 km than lower levels. The aerosol type occurrence frequency has large seasonal variations in this region. The altitude of the peak occurrence frequency of the dust layer top is nearly the same as that of all-aerosol in MAM and JJA.

[43] 5. In SE Asia, aerosol properties do not show much seasonal variation. Throughout the year, clean marine aerosol is the dominant type detected below 4 km. The altitude of the peak occurrence frequency of the aerosol layer top is ~7 km for all-aerosol and ~1–2 km for dust.

[44] *Desert regime*:

[45] 1. Dust is the dominant type detected from the surface to the middle troposphere and sometimes can extend to above 8 km.

[46] 2. Dust contributes significantly to all-aerosol extinction at nearly all levels. The dust layer top has nearly the same altitude of the peak occurrence frequency as all aerosol.

[47] 3. West Australia is an exception. The detected aerosol characteristics in this region are closer to the biomass burning regime rather than the desert regime.

[48] 4. A notable common feature in northern Africa and west China is a secondary peak of the layer top occurrence frequency of all-aerosol, which is detected at ~18 km only during JJA, suggesting the existence of an aerosol layer at the tropopause level during boreal summer.

[49] 5. In northern Africa, the largest extinction near the surface is detected in JJA. Dust is the dominant type with a constant occurrence frequency more than 50% detected at ~1–4 km during all seasons except DJF.

[50] 6. In west China, the overlap of dust and all-aerosol extinction profiles only occurs in MAM. A secondary peak of dust extinction is detected around 2.5 km during MAM and JJA. During MAM, dust can reach as high as 11 km, and the altitude of the peak occurrence frequency of the dust layer top is the same as that of all-aerosol.

[51] *Fossil fuel and industry regime*:

[52] 1. The dominant aerosol types detected include polluted dust, smoke, and dust, with each type dominating at different levels. The dominant aerosol types also have large geographical and seasonal variations.

[53] 2. Dust contribution to all-aerosol extinction is highly dependent on the location and season. If big desert areas are included in the domain or nearby, dust can play an important role during some specific periods. During other periods, dust

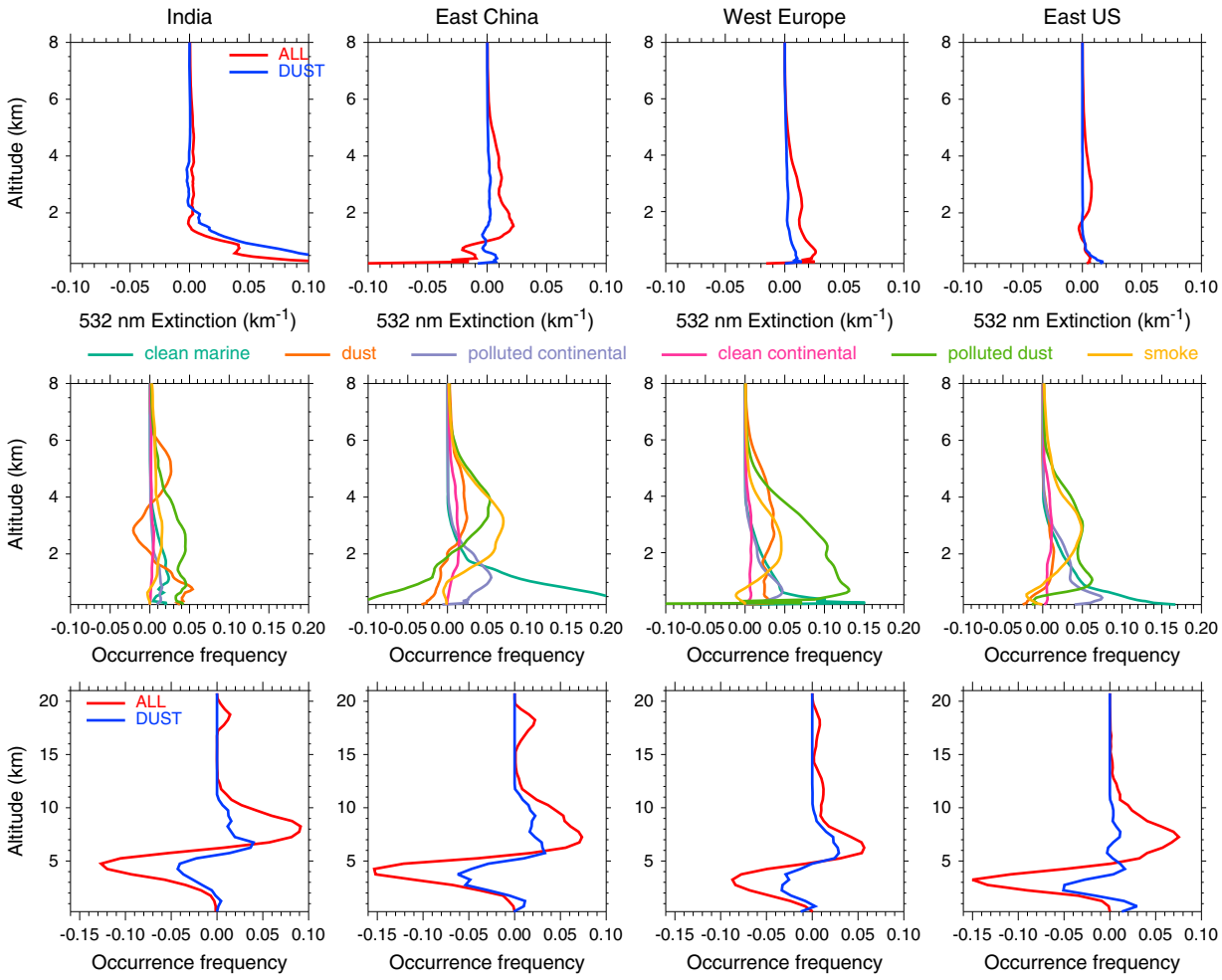

Figure 16. Same as Figure 14 but over (left) India, (second column from left) east China, (third column from left) west Europe, and (right) East U.S.

has little impact on the all-aerosol extinction, and the dust layer top has a lower altitude of the peak occurrence frequency than that of all-aerosol.

[54] 3. A notable feature is detected over India and east China, i.e., a distinct secondary peak occurrence frequency of the all-aerosol layer top at ~18 km only during JJA.

[55] 4. In India, the extinction profile of dust is close to that of all-aerosol in MAM and JJA, and dust reaches a higher altitude than in other seasons. Dust is the most often detected type from near the surface to as high as 10 km in MAM.

[56] 5. In east China, the dust extinction profile is close to the all-aerosol extinction profile only in MAM. Dust is detected as the dominant type above 2 and 3 km in MAM and DJF, respectively, and can reach as high as 11 km during MAM.

[57] 6. In west Europe, dust is detected to contribute more to all-aerosol extinction in the upper level than the lower level during MAM and JJA. Dust (polluted dust) is detected predominantly above (below) 3 km in nearly all seasons. Aerosols are classified as smoke less often than dust and polluted dust in this region.

[58] 7. In East U.S., dust contributes little to all-aerosol extinction. Polluted dust is detected predominantly in the lower to middle troposphere and can reach as high as 10 km in MAM and JJA. Smoke is detected predominantly above 5 km during JJA and SON.

[59] *Oceanic regime*:

[60] 1. The dominant aerosol types detected include clean marine, dust, polluted dust, and smoke; clean marine dominates near the ocean surface, while the other three types have large geographical and seasonal variations.

[61] 2. Dust contribution to all-aerosol extinction is small or only limited to the upper level. The dust layer top has a lower altitude of the peak occurrence frequency than that of all-aerosol. Two exceptions are NW Pacific in MAM and central Atlantic in MAM/JJA. The former is related to the strong trans-Pacific transport of dust in the middle to upper troposphere from Asia, and the latter is associated with dust output from the nearby Sahara desert.

[62] 3. Over NW Pacific, polluted dust is detected as the dominant type from ~1 to 4 km, and dust dominates at 4–9 km in MAM. Smoke plays an important role above 3 km in JJA and SON. During DJF, dust becomes the dominant type detected from 5 to 9 km.

[63] 4. Over North Atlantic, dust is the dominant type detected at 2.5–4.5 km during JJA and SON, while smoke

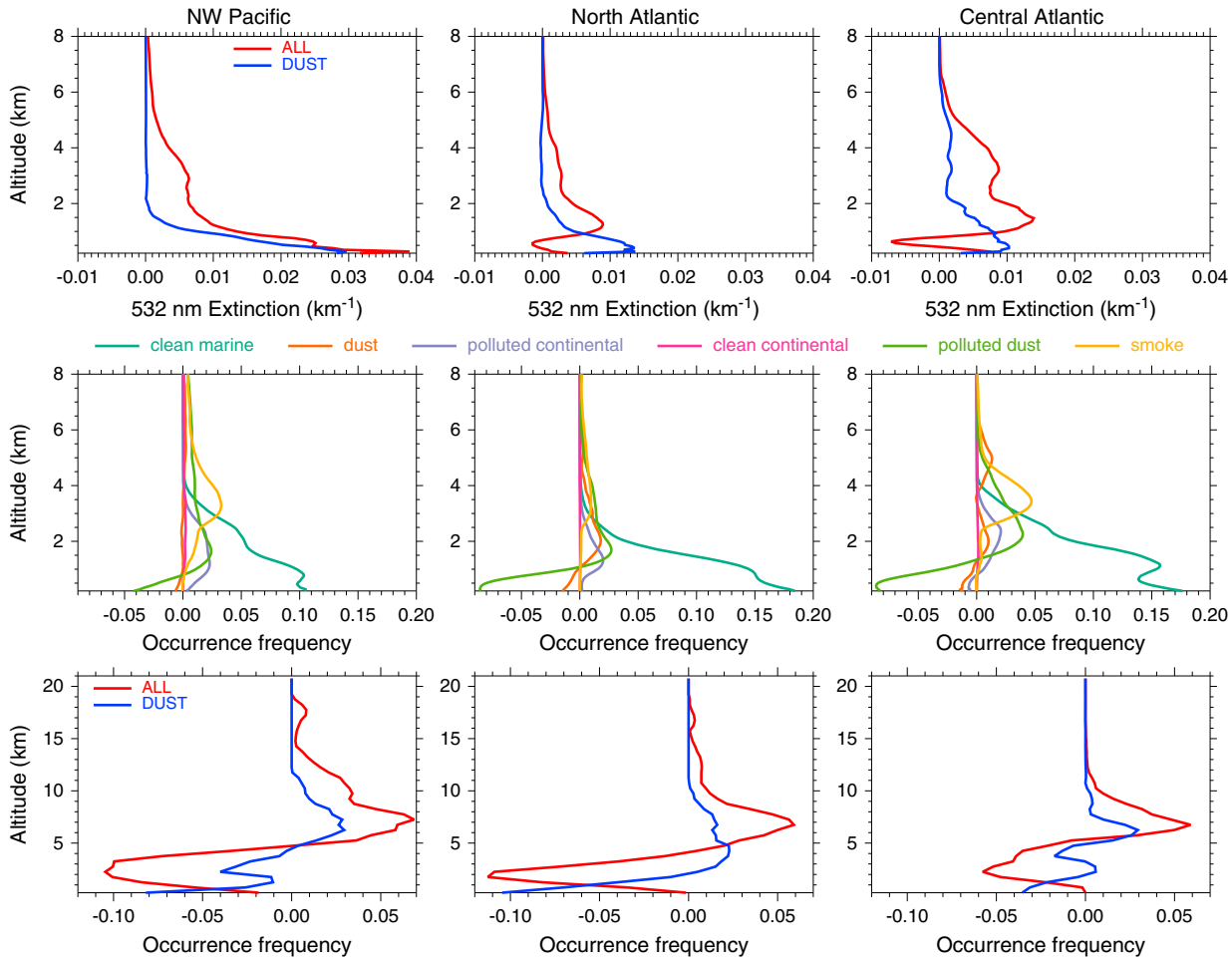

Figure 17. Same as Figure 14 but over (left) northwest Pacific, (middle) North Atlantic, and (right) central Atlantic.

dominates above 4.5 km. In MAM, dust and polluted dust are the dominant types detected above 3 km, while in DJF, smoke becomes the dominant type detected above 3 km.

[64] 5. Over central Atlantic, the extinction profile of dust is much closer to that of all-aerosol in the upper level than the lower level during MAM and JJA. Dust is detected as the dominant type only in MAM and JJA at 2–6 km. Smoke is detected most often above 6 km in all seasons, and its dominance can extend downward to 3 km in SON.

[65] In general, the nighttime minus daytime differences of aerosol properties do not show much seasonal variation except for a few cases. Within the same aerosol regime, the diurnal variation is similar. The main points of diurnal variations of aerosol properties are summarized in the following.

[66] 1. All-aerosol extinction is larger during nighttime, while dust extinction shows little diurnal variation except when dust dominates in the aerosol composition.

[67] 2. Smoke is detected more frequently from the lower to middle troposphere during nighttime. Clean marine and polluted continental aerosols are detected more frequently, while polluted dust is detected less frequently, in the lower troposphere during nighttime.

[68] 3. The aerosol layer top is detected at high altitudes more frequently during nighttime. The dust layer top shows a much smaller diurnal variation than the all-aerosol layer top and could be detected slightly more frequently near the surface during nighttime than daytime.

[69] Although the Version 1.0 Level 3 aerosol profile product is a beta release [*CALIPSO*, 2011], our analyses of this data set suggest that the seasonal and diurnal variations of aerosol vertical distributions look qualitatively reasonable in most regions in terms of extinction coefficient, aerosol type, and maximum aerosol layer top altitude. More dedicated efforts of improving CALIPSO retrieval algorithms are needed to produce aerosol extinction profiles with much improved quality in the future.

Appendix: Number of Aerosol Samples

[70] The profiles of the total number of aerosol samples (after data screening) detected by CALIPSO over each region are shown in the Figures A1–A4, corresponding to the four aerosol regimes discussed in the main text. Generally, CALIPSO detects more aerosol samples during nighttime than daytime, especially in the middle to upper troposphere, which is due to the solar impact on the aerosol detection sensitivity. Fewer aerosol samples are detected at high altitudes than near the surface.

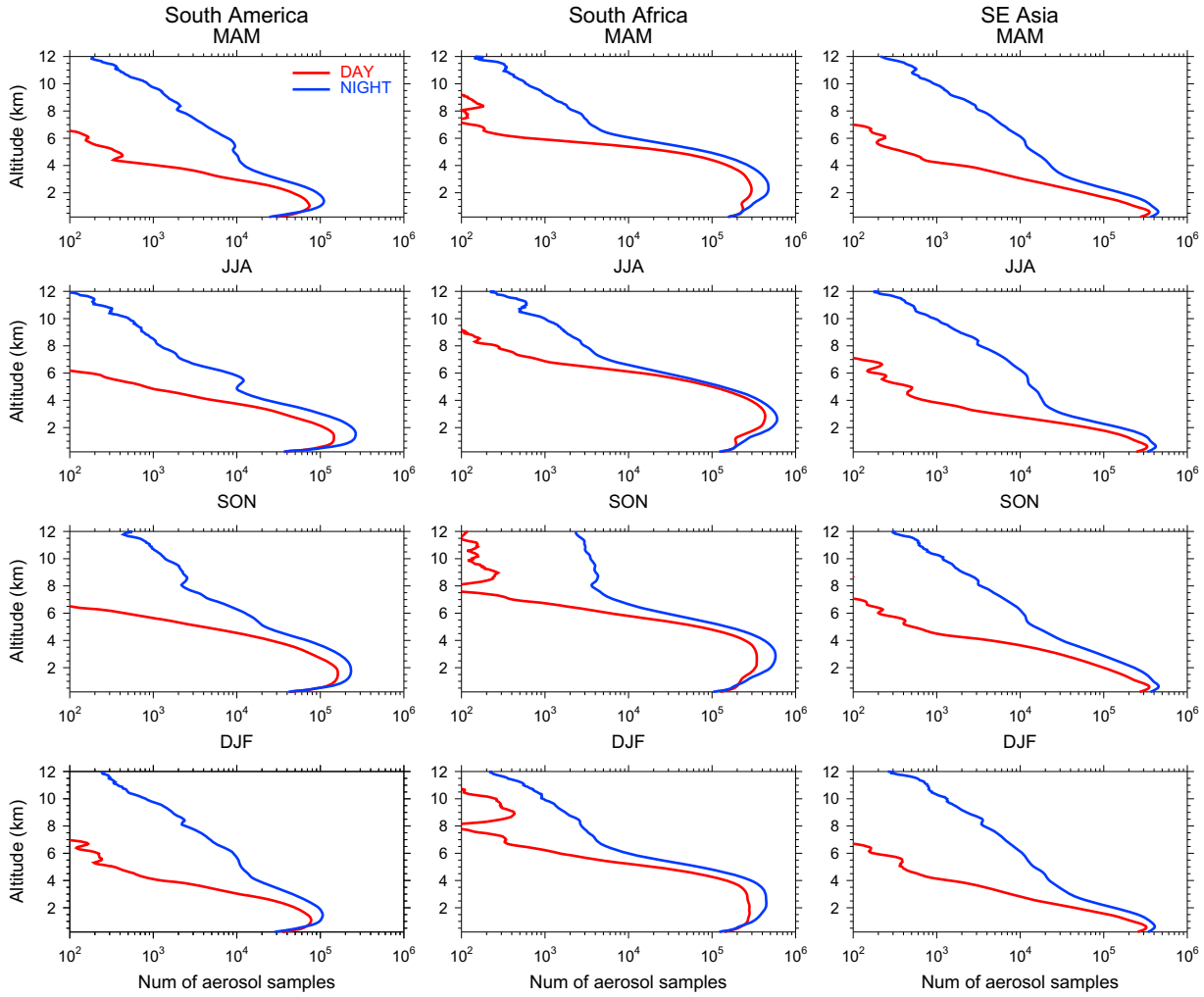

Figure A1. Vertical profiles of the 5-year total number of aerosol samples detected by CALIPSO over (left) South America, (middle) southern Africa, and (right) Southeast Asia. From top to bottom are seasonal total numbers for boreal spring (MAM), summer (JJA), fall (SON), and winter (DJF), respectively. The red curve represents daytime observations, and the blue curve represents nighttime observations.

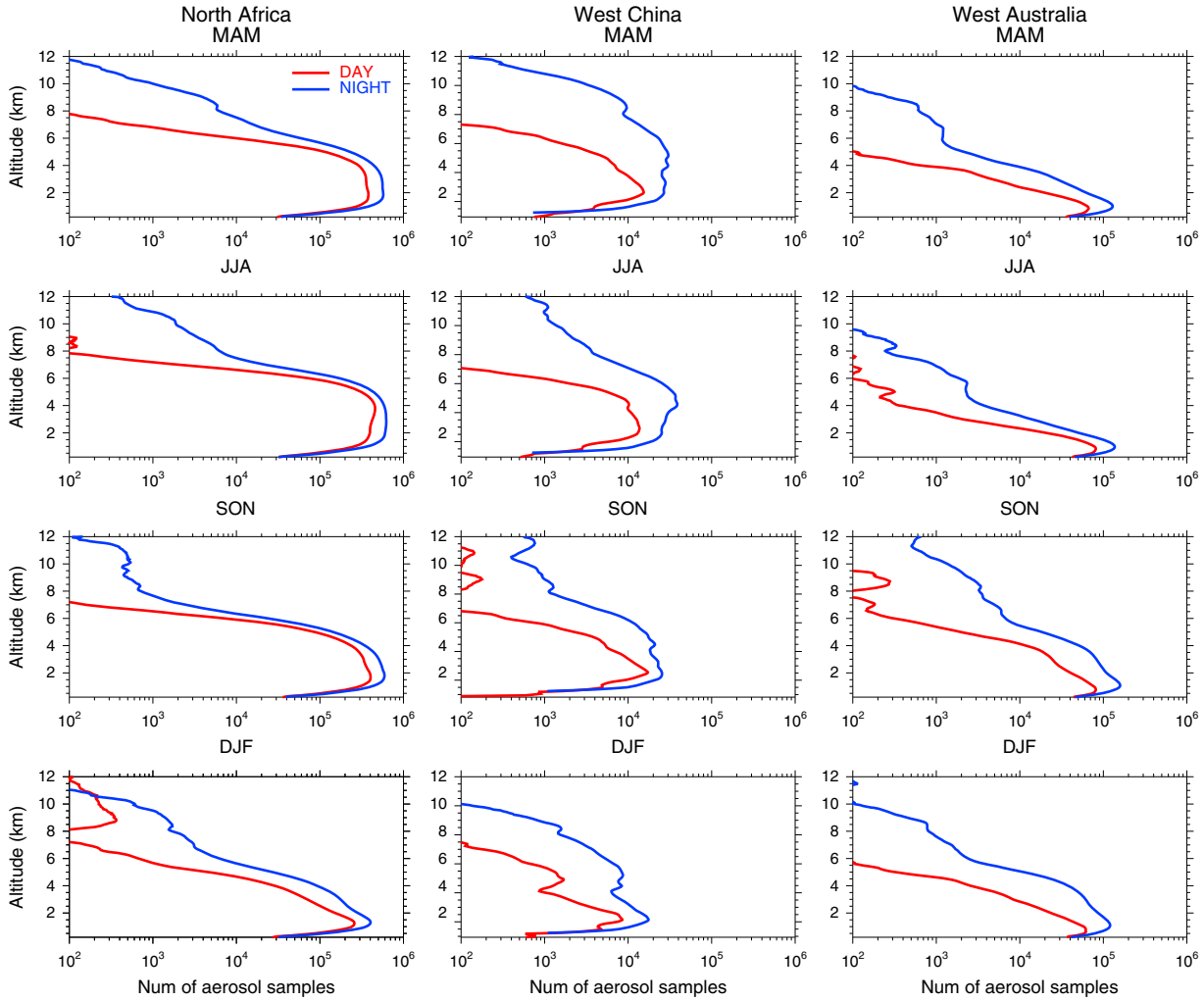

Figure A2. Same as Figure A1 but over (left) northern Africa, (middle) west China, and (right) west Australia.

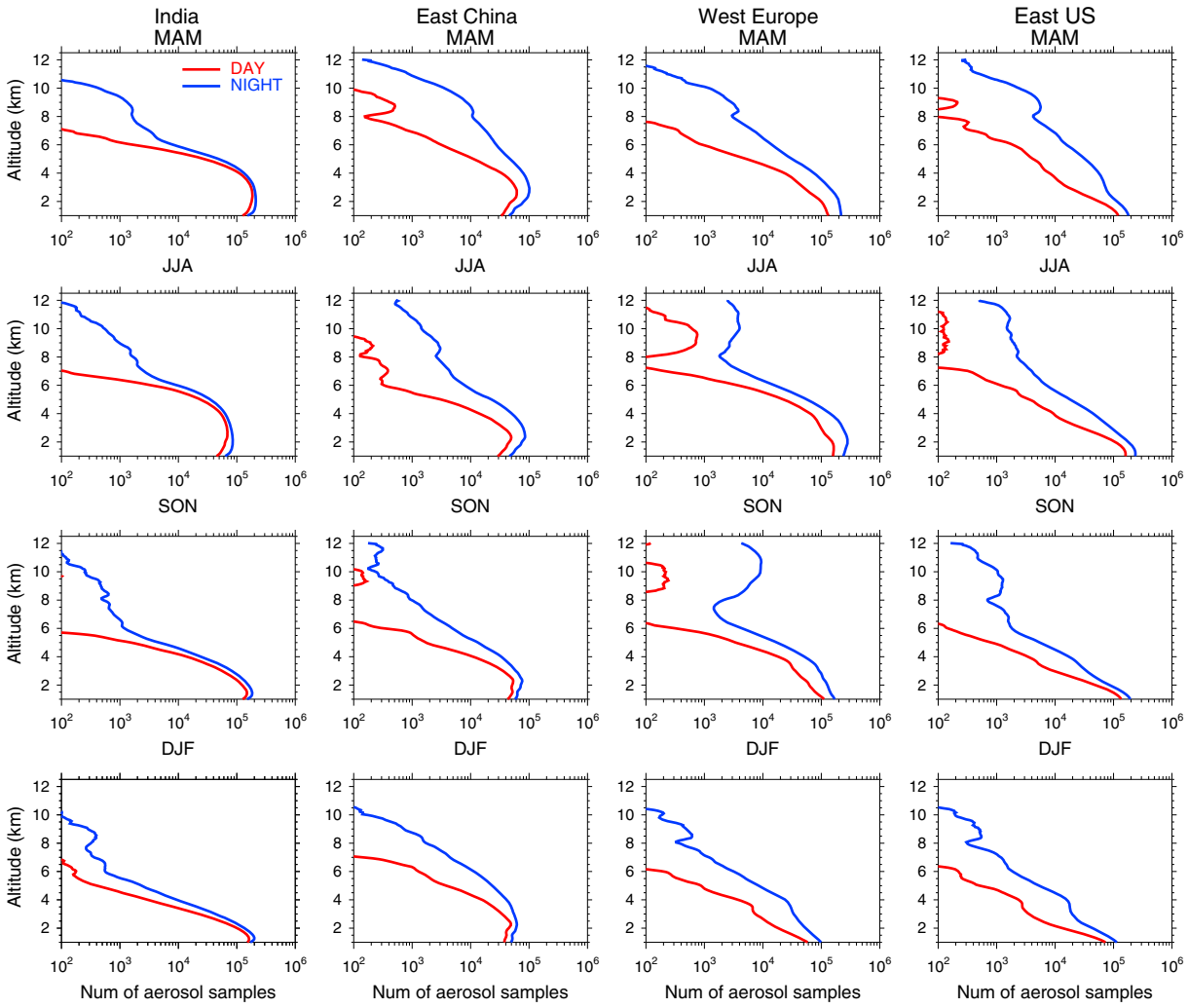

Figure A3. Same as Figure A1 but over (left) India, (second column from left) east China, (third column from left) west Europe, and (right) East U.S.

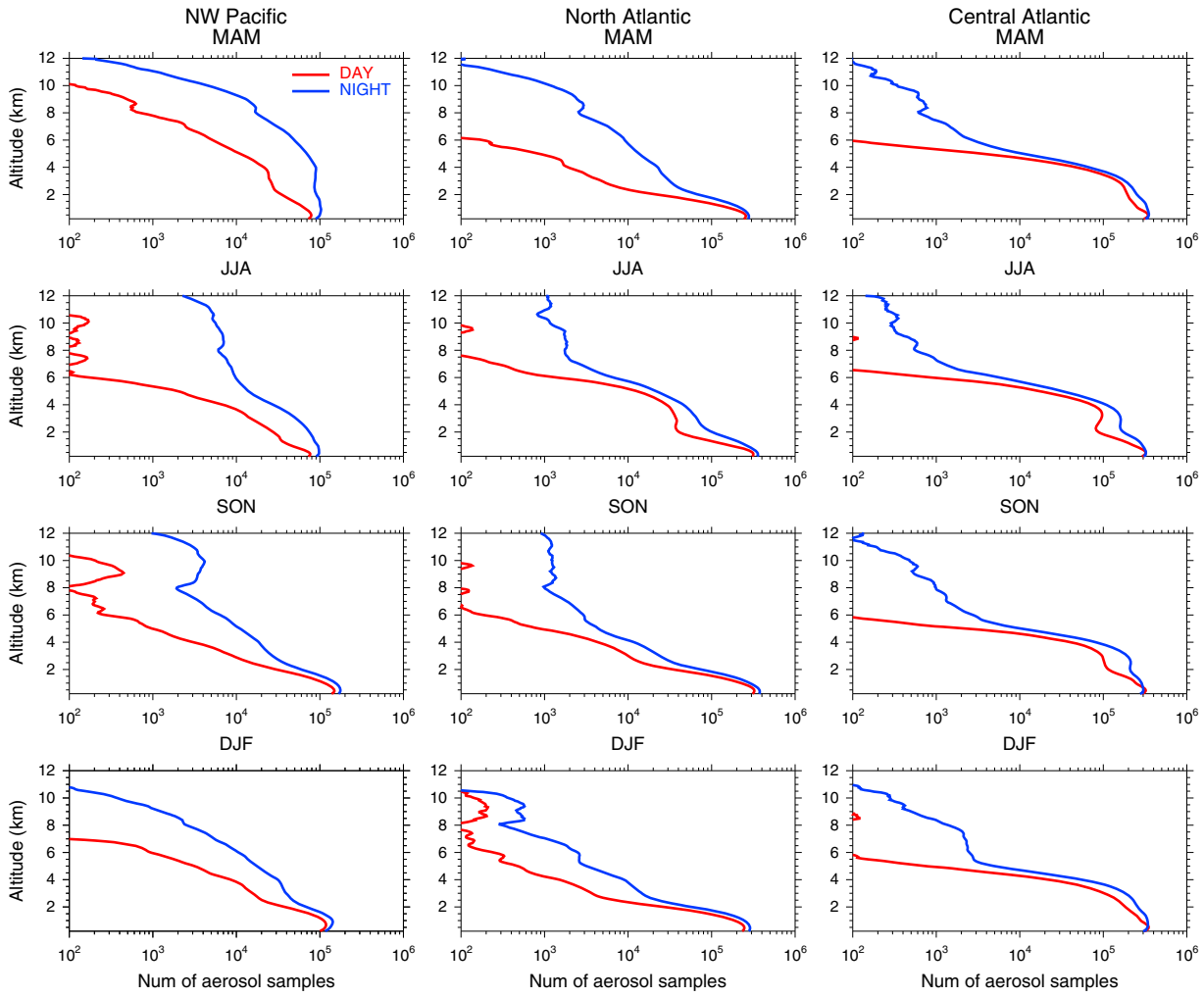

Figure A4. Same as Figure A1 but over (left) northwest Pacific, (middle) North Atlantic, and (right) central Atlantic.

[71] **Acknowledgments.** This research was supported by the NASA Aura Science Team program (NNX11AE72G) and the Jackson School of Geosciences at the University of Texas at Austin. Most of this study was performed at NASA Jet Propulsion Laboratory (JPL) at the California Institute of Technology, under contract with NASA. The first author thanks support from the JPL Graduate Fellowship Program. The third author would like to thank Ali Omar and Stuart Young for input on CALIPSO aerosol typing. We also appreciate the comments from four anonymous reviewers that led to significant improvements of this paper. The CALIPSO Level 3 data were obtained from the Atmospheric Science Data Center at NASA Langley Research Center.

References

Ackerman, A. S., O. B. Toon, D. E. Stevens, A. J. Heymsfield, V. Ramanathan, and E. J. Welton (2000), Reduction of tropical cloudiness by soot, *Science*, *288*(5468), 1042–1047, doi:10.1126/science.288.5468.1042.

Bou Karam, D., C. Flamant, J. Cuesta, J. Pelon, and E. Williams (2010), Dust emission and transport associated with a Saharan depression: February 2007 case, *J. Geophys. Res.*, *115*, D00H27, doi:10.1029/2009JD012390.

CALIPSO (2010), CALIPSO Quality Statements: Lidar Level 2 Cloud and Aerosol Profile Products Version Releases 3.01 and 3.02, available at http://eosweb.larc.nasa.gov/PRODOCS/calipso/Quality_Summaries/CALIOP_L2ProfileProducts_3.01.html, accessed on 30 January 2013.

CALIPSO (2011), CALIPSO Quality Statements Lidar Level 3 Aerosol Profile Monthly Products Version Release 1.00, available at http://eosweb.larc.nasa.gov/PRODOCS/calipso/Quality_Summaries/CALIOP_L3AProProducts_1-00.html, accessed on 15 July 2012.

Charlson, R. J., S. E. Schwartz, J. M. Hales, R. D. Cess, J. A. Coakley, J. E. Hansen, and D. J. Hofmann (1992), Climate forcing by anthropogenic aerosols, *Science*, *255*(5043), 423–430, doi:10.1126/science.255.5043.423.

Chazette, P. (2003), The monsoon aerosol extinction properties at Goa during INDOEX as measured with lidar, *J. Geophys. Res.*, *108*(D6), 4187, doi:10.1029/2002JD002074.

Dai, A. (2001), Global precipitation and thunderstorm frequencies. Part II: Diurnal variations, *J. Clim.*, *14*(6), 1112–1128.

Dai, A., F. Giorgi, and K. E. Trenberth (1999), Observed and model-simulated diurnal cycles of precipitation over the contiguous United States, *J. Geophys. Res.*, *104*(D6), 6377–6402, doi:10.1029/98JD02720.

Damoah, R., N. Spichtinger, C. Forster, P. James, I. Mattis, U. Wandinger, S. Beirle, T. Wagner, and A. Stohl (2004), Around the world in 17 days—Hemispheric-scale transport of forest fire smoke from Russia in May 2003, *Atmos. Chem. Phys.*, *4*, 1311–1321, doi:10.5194/acp-4-1311-2004.

Duncan, B. N., R. V. Martin, A. C. Staudt, R. Yevich, and J. A. Logan (2003), Interannual and seasonal variability of biomass burning emissions constrained by satellite observations, *J. Geophys. Res.*, *108*(D2), 4100, doi:10.1029/2002JD002378.

Duncan, B. N., J. A. Logan, I. Bey, I. A. Megretskaia, R. M. Yantosca, P. C. Novelli, N. B. Jones, and C. P. Rinsland (2007), Global budget of CO, 1988–1997: Source estimates and validation with a global model, *J. Geophys. Res.*, *112*, D22301, doi:10.1029/2007JD008459.

Dwyer, E., S. Pinnock, J. M. Gregoire, and J. M. C. Pereira (2000), Global spatial and temporal distribution of vegetation fire as determined from satellite observations, *Int. J. Remote Sens.*, *21*, 1289–1302.

Eguchi, K., I. Uno, K. Yumimoto, T. Takemura, A. Shimizu, N. Sugimoto, and Z. Liu (2009), Trans-pacific dust transport: integrated analysis of

NASA/CALIPSO and a global aerosol transport model, *Atmos. Chem. Phys.*, *9*, 3137–3145, doi:10.5194/acp-9-3137-2009.

Generoso, S., I. Bey, M. Labonne, and F. M. Breon (2008), Aerosol vertical distribution in dust outflow over the Atlantic: Comparisons between GEOS-Chem and Cloud-Aerosol Lidar and Infrared Pathfinder Satellite Observation (CALIPSO), *J. Geophys. Res.*, *113*, D24209, doi:10.1029/2008JD010154.

Giglio, L., I. Csiszar, and C. O. Justice (2006), Global distribution and seasonality of active fires as observed with the Terra and Aqua Moderate Resolution Imaging Spectroradiometer (MODIS) sensors, *J. Geophys. Res.*, *111*, G02016, doi:10.1029/2005JG000142.

Hains, J. C., B. F. Taubman, A. M. Thompson, J. W. Stehr, L. T. Marufu, B. G. Doddridge, and R. R. Dickerson (2008), Origins of chemical pollution derived from Mid-Atlantic aircraft profiles using a clustering technique, *Atmos. Environ.*, *42*, 1727–1741, doi:10.1016/j.atmosenv.2007.11.052.

Haywood, J. M., and V. Ramaswamy (1998), Global sensitivity studies of the direct radiative forcing due to anthropogenic sulfate and black carbon aerosols, *J. Geophys. Res.*, *103*(D6), 6043–6058, doi:10.1029/97JD03426.

Huang, J., Q. Fu, J. Su, Q. Tang, P. Minnis, Y. Hu, Y. Yi, and Q. Zhao (2009), Taklimakan dust aerosol radiative heating derived from CALIPSO observations using the Fu-Liou radiation model with CERES constraints, *Atmos. Chem. Phys.*, *9*, 4011–4021, doi:10.5194/acp-9-4011-2009.

Huang, Z. W., J. P. Huang, J. R. Bi, G. Y. Wang, W. C. Wang, Q. A. Fu, Z. Q. Li, S. C. Tsay, and J. S. Shi (2010), Dust aerosol vertical structure measurements using three MPL lidars during 2008 China-US joint dust field experiment, *J. Geophys. Res.*, *115*, D00K15, doi:10.1029/2009JD013273.

Huang, L., R. Fu, J. H. Jiang, J. S. Wright, and M. Luo (2012), Geographic and seasonal distributions of CO transport pathways and their roles in determining CO centers in the upper troposphere, *Atmos. Chem. Phys.*, *12*, 4683–4698, doi:10.5194/acp-12-4683-2012.

Husar, R. B., et al. (2001), Asian dust events of April 1998, *J. Geophys. Res.*, *106*(D16), 18,317–18,330, doi:10.1029/2000JD900788.

Intergovernmental Panel on Climate Change (IPCC) (2007), *Climate Change 2007: Synthesis Report. Contribution of Working Groups I, II and III to the Fourth Assessment Report of the Intergovernmental Panel on Climate Change*, edited by Core Writing Team, Pachauri, R. K., and A. Reisinger, 104 pp., IPCC, Geneva, Switzerland.

Jiang, H. L., and G. Feingold (2006), Effect of aerosol on warm convective clouds: Aerosol-cloud-surface flux feedbacks in a new coupled large eddy model, *J. Geophys. Res.*, *111*, D01202, doi:10.1029/2005JD006138.

Jiang, J. H., H. Su, M. R. Schoeberl, S. T. Massie, P. Colarco, S. Platnick, and N. J. Livesey (2008), Clean and polluted clouds: Relationships among pollution, ice clouds, and precipitation in South America, *Geophys. Res. Lett.*, *35*, L14804, doi:10.1029/2008GL034631.

Kacenelenbogen, M., M. A. Vaughan, J. Redemann, R. M. Hoff, R. R. Rogers, R. A. Ferrare, P. B. Russell, C. A. Hostetler, J. W. Hair, and B. N. Holben (2011), An accuracy assessment of the CALIOP/CALIPSO version 2/version 3 daytime aerosol extinction product based on a detailed multi-sensor, multi-platform case study, *Atmos. Chem. Phys.*, *11*(8), 3981–4000, doi:10.5194/acp-11-3981-2011.

Kaufman, Y. J., J. M. Haywood, P. V. Hobbs, W. Hart, R. Kleidman, and B. Schmid (2003), Remote sensing of vertical distributions of smoke aerosol off the coast of Africa, *Geophys. Res. Lett.*, *30*(16), 1831, doi:10.1029/2003GL017068.

Koffi, B., et al. (2012), Application of the CALIOP layer product to evaluate the vertical distribution of aerosols estimated by global models: AeroCom phase I results, *J. Geophys. Res.*, *117*(D10), D10201, doi:10.1029/2011JD016858.

Koren, I., Y. J. Kaufman, L. A. Remer, and J. V. Martins (2004), Measurement of the effect of Amazon smoke on inhibition of cloud formation, *Science*, *303*(5662), 1342–1345, doi:10.1126/science.1089424.

Koren, I., J. V. Martins, L. A. Remer, and H. Afargan (2008), Smoke invigoration versus inhibition of clouds over the Amazon, *Science*, *321*(5891), 946–949, doi:10.1126/science.1159185.

L'Ecuyer, T. S., and J. H. Jiang (2010), Touring the atmosphere aboard the A-Train, *Phys. Today*, *63*(7), 36–41, doi:10.1063/1.3463626.

Li, S. M., A. M. Macdonald, J. W. Strapp, Y. N. Lee, and X. L. Zhou (1997), Chemical and physical characterizations of atmospheric aerosols over southern California, *J. Geophys. Res.*, *102*(D17), 21,341–21,353, doi:10.1029/97JD01310.

Liu, P. F., C. S. Zhao, Q. Zhang, Z. Z. Deng, M. Y. Huang, X. C. Ma, and X. X. Tie (2009a), Aircraft study of aerosol vertical distributions over Beijing and their optical properties, *Tellus, Ser. B*, *61*(5), 756–767, doi:10.1111/j.1600-0889.2009.00440.x.

Liu, Z. Y., M. Vaughan, D. Winker, C. Kittaka, B. Getzewich, R. Kuehn, A. Omar, K. Powell, C. Trepte, and C. Hostetler (2009b), The CALIPSO lidar cloud and aerosol discrimination: Version 2 algorithm and initial assessment of performance, *J. Atmos. Oceanic Technol.*, *26*, 1198–1213, doi:10.1175/2009JTECHA1229.1.

Matthias, V., et al. (2004), Vertical aerosol distribution over Europe: Statistical analysis of Raman lidar data from 10 European Aerosol Research Lidar Network (EARLINET) stations, *J. Geophys. Res.*, *109*, D18201, doi:10.1029/2004JD004638.

Miller, S. T. K., B. D. Keim, R. W. Talbot, and H. Mao (2003), Sea breeze: Structure, forecasting, and impacts, *Rev. Geophys.*, *41*(3), 1011, doi:10.1029/2003RG000124.

Nesbitt, S. W., and E. J. Zipser (2003), The diurnal cycle of rainfall and convective intensity according to three years of TRMM measurements, *J. Clim.*, *16*(10), 1456–1475, doi:10.1175/1520-0442(2003)016.

Omar, A. H., et al. (2009), The CALIPSO automated aerosol classification and lidar ratio selection algorithm, *J. Atmos. Oceanic Technol.*, *26*(10), 1994–2014, doi:10.1175/2009JTECHA1231.1.

Osborne, S. R., and J. M. Haywood (2005), Aircraft observations of the microphysical and optical properties of major aerosol species, *Atmos. Res.*, *73*(3–4), 173–201.

Powell, K., et al. (2011), Cloud-Aerosol LIDAR Infrared Pathfinder Satellite Observations (CALIPSO) Data Management System Data Products Catalog, Document No. PC-SCI-503, Release 3.4, NASA Langley Research Center, Hampton, Va.

Prospero, J. M., P. Ginoux, O. Torres, S. E. Nicholson, and T. E. Gill (2002), Environmental characterization of global sources of atmospheric soil dust identified with the NIMBUS 7 Total Ozone Mapping Spectrometer (TOMS) absorbing aerosol product, *Rev. Geophys.*, *40*(1), 1002, doi:10.1029/2000RG000095.

Redemann, J., M. A. Vaughan, Q. Zhang, Y. Shinozuka, P. B. Russell, J. M. Livingston, M. Kacenelenbogen, and L. A. Remer (2012), The comparison of MODIS-Aqua (C5) and CALIOP (V2 & V3) aerosol optical depth, *Atmos. Chem. Phys.*, *12*(6), 3025–3043, doi:10.5194/acp-12-3025-2012.

Rozwadowska, A. (2007), Influence of aerosol vertical profile variability on retrievals of aerosol optical thickness from NOAA AVHRR measurements in the Baltic region, *Oceanologia*, *49*(2), 165–184.

Sekiyama, T. T., T. Y. Tanaka, A. Shimizu, and T. Miyoshi (2010), Data assimilation of CALIPSO aerosol observations, *Atmos. Chem. Phys.*, *10*, 39–49, doi:10.5194/acp-10-39-2010.

Shinozuka, Y., A. D. Clarke, S. G. Howell, V. N. Kapustin, C. S. McNaughton, J. C. Zhou, and B. E. Anderson (2007), Aircraft profiles of aerosol microphysics and optical properties over North America: Aerosol optical depth and its association with PM2.5 and water uptake, *J. Geophys. Res.*, *112*, D12S20, doi:10.1029/2006JD007918.

Soden, B. J. (2000), The diurnal cycle of convection, clouds, and water vapor in the tropical upper troposphere, *Geophys. Res. Lett.*, *27*(15), 2173–2176, doi:10.1029/2000GL011436.

Sorooshian, A., and H. T. Duong (2010), Ocean emission effects on aerosol-cloud interactions: Insights from two case studies, *Adv. Meteorol.*, *2010*, 301–395, doi:10.1155/2010/301395.

Twomey, S. (1977), The influence of pollution on the shortwave albedo of clouds, *J. Atmos. Sci.*, *34*, 1149–1152.

Vernier, J. P., L. W. Thomason, and J. Kar (2011), CALIPSO detection of an Asian tropopause aerosol layer, *Geophys. Res. Lett.*, *38*, L07804, doi:10.1029/2010GL046614.

van der Werf, G. R., J. T. Randerson, G. J. Collatz, and L. Giglio (2003), Carbon emissions from fires in tropical and subtropical ecosystems, *Global Change Biol.*, *9*(4), 547–562, doi:10.1046/j.1365-2486.2003.00604.x.

Winker, D. M., W. H. Hunt, and M. J. McGill (2007), Initial performance assessment of CALIOP, *Geophys. Res. Lett.*, *34*, L19803, doi:10.1029/2007GL030135.

Winker, D. M., M. A. Vaughan, A. Omar, Y. X. Hu, K. A. Powell, Z. Y. Liu, W. H. Hunt, and S. A. Young (2009), Overview of the CALIPSO mission and CALIOP data processing algorithms, *J. Atmos. Oceanic Technol.*, *26*, 2310–2323, doi:10.1175/2009JTECHA1281.1.

Winker, D., J. Tackett, B. Getzewich, Z. Liu, M. Vaughan, and R. Rogers (2012), The global 3-D distribution of tropospheric aerosols as characterized by CALIOP, *Atmos. Chem. Phys. Discuss*, *12*, 24,847–24,893, doi:10.5194/acpd-12-24847-2012.

Young, S. A., and M. A. Vaughan (2009), The retrieval of profiles of particulate extinction from Cloud Aerosol Lidar Infrared Pathfinder Satellite Observations (CALIPSO) data: Algorithm description, *J. Atmos. Oceanic Technol.*, *26*, 1105–1119, doi:10.1175/2008 JTECHA1221.1.

Yu, H. B., M. Chin, D. M. Winker, A. H. Omar, Z. Y. Liu, C. Kittaka, and T. Diehl (2010), Global view of aerosol vertical distributions from CALIPSO lidar measurements and GOCART simulations: Regional and seasonal variations, *J. Geophys. Res.*, *115*, D00H30, doi:10.1029/2009JD013364.